ストレスの分子免疫学的評価方法開発に関する研究

平成５～７年度　特別研究報告書

労働省産業医学総合研究所

ストレスの分子免疫学的評価方法開発に関する研究

特別研究報告書

研究担当　三枝　順三
久保田　久代

研究期間　平成５～７年度

Industrial Health, 1996, **34**, 139—142

Antinucleolar Autoantibody Induced by Mercuric Chloride in Mice: Does Sodium Selenite Inhibit Autoantibody Production?

Abstract: Repeated exposure of subtoxic doses of mercuric chloride ($HgCl_2$) can induce antinucleolar autoantibodies in susceptible mice. To study the immunopathological mechanism(s), sodium selenite (Na_2SeO_3), which is known to reduce the toxicity of mercury, is injected simultaneously with $HgCl_2$ into mice. Equimolar Na_2SeO_3 nor the same amount of Se in Na_2SeO_3 as Hg in $HgCl_2$ could not reduce antinucleolar autoantibody induction by $HgCl_2$. These results indicate that the mechanism of autoimmunity induction by $HgCl_2$ might be independent of its toxicity.

Key words: $HgCl_2$ — Na_2SeO_3 — Antinucleolar autoantibody

Chronic exposure to metals and their compounds is associated with severe toxic effects. While often overlooked, several metals are frequently responsible for immunological reactions, resulting in allergic contact dermatitis and/or autoimmunity in individuals who come into contact with metal products occupationally[1].

Experimental models of metal-induced hypersensitivity including autoimmunity have been developed. Repeated exposure to subtoxic doses of mercuric chloride ($HgCl_2$) can induce anti-glomerular basement membrane antibodies or antinuclear antibodies in rats and rabbits, resulting in severe autoimmune or immune complex glomerulonephritis[2–4]. $HgCl_2$ also induces antinucleolar autoantibodies (AnuA) in susceptible mice[5–8]. These immunological abnormalities occur in a T cell dependent manner[8–11]. The susceptibility to $HgCl_2$ induced autoimmunity is mainly determined by the class II major histocompatibility complexes (MHC), though extra MHC genes may also be involved[2, 12–15]. In addition, $HgCl_2$ increases the expression of class II MHC on B cells in rats and mice[16–18].

Sodium selenite (Na_2SeO_3) protects against the toxicity of $HgCl_2$. Necrotizing changes of renal tubules caused by $HgCl_2$ toxicity completely disappeared after the administration of Na_2SeO_3[19]. Further, animals given a lethal dose of $HgCl_2$ together with Na_2SeO_3 survived with few pathological changes[19, 20]. However, its effect on autoimmunity induction by $HgCl_2$ had not yet been studied. Thus, we performed the present experiments.

IQI/Jcl mice were obtained from the Central Institute for Experimental Animals (Kawasaki, Japan), and were maintained in our own animal facilities under conventional conditions. Both male and female mice were supplied for the experiments at 8 to 10 weeks old.

Stock solutions of 10 mg/ml of $HgCl_2$ (Wako Pure Chemical, Tokyo, Japan) and Na_2SeO_3 (Wako Pure Chemical, Tokyo, Japan) in sterile 0.9% saline were prepared

at the beginning of each experiment. Before administration, aliquot of the stock solutions were diluted with sterile 0.9% saline to the desired concentrations. To avoid direct contact, mice simultaneously received subcutaneous injection of 0.1 ml $HgCl_2$ solution and intraperitoneal injection of 0.5 ml Na_2SeO_3 solution 3 times a week for 4 weeks. Control mice were given subcutaneous 0.1 ml and/or intraperitoneal 0.5 ml of 0.9% saline.

The mice were anesthetized with chloroform and then bled by heart puncture 2 days after the final injection. Sera were separated and stored at -20°C until use. AnuA levels were determined by indirect immuno-fluorescence using rat myoid cells (R615B2) as the substrate and fluorescein-conjugated goat-anti-mouse IgG (Cappel, West Chester, PA, USA). The sera were diluted with phosphate buffered saline by a 2-fold dilution starting at 1:10. The AnuA titer was expressed as the number of the tube with the highest dilution showing the nucleolar staining. Details of the method were described previously[8].

Since Na_2SeO_3 can reduce the toxic effects of $HgCl_2$ and its optimum suppressive effects occur when equimolar amounts are administered[20], equimolar amounts of $HgCl_2$ and Na_2SeO_3 were injected at the first experiment. Repeated administration of 4 μmole/kg (1.09 mg/kg) $HgCl_2$ induced high titer AnuA in all mice with and without injection of 4 μmole/kg (0.69 mg/kg) Na_2SeO_3 (Table 1). Injection of Na_2SeO_3 alone did not induce any AnuA. In the second experiment, the same amounts of metals were administered. Male mice were injected with 1 mg/kg $HgCl_2$ (0.74 mg/kg as Hg) and 1.84 mg/kg Na_2SeO_3 (0.74 mg/kg as Se), or 0.25 mg/kg $HgCl_2$ (0.19 mg/kg as Hg) and 0.46 mg/kg Na_2SeO_3 (0.19 mg/kg as Se), respectively. Once again, Na_2SeO_3 did not inhibit AnuA induction by $HgCl_2$ (Table 2).

In these experiments, neither simultaneous injection with equimolar Na_2SeO_3 nor amounts of Se equivalent to Hg reduced AnuA induction by $HgCl_2$. These results

Table 1. Effects of Na_2SeO_3 on AnuA induction by $HgCl_2$ (I).

Sex	Treatment	Positive/Examined	Titer
Male	Saline + Saline	0/8	
	Saline + Na_2SeO_3	0/8	
	$HgCl_2$ + Saline	8/8	7.5 ± 0.9
	$HgCl_2$ + Na_2SeO_3	10/10	7.5 ± 0.5
Female	Saline + Saline	0/7	
	Saline + Na_2SeO_3	0/7	
	$HgCl_2$ + Saline	7/7	6.7 ± 1.5
	$HgCl_2$ + Na_2SeO_3	7/7	7.6 ± 0.5

4 μmol/kg $HgCl_2$ (0.1 ml/mouse, *s.c.*) and/or 4 μmole/kg Na_2SeO_3 (0.5 ml/mouse, *i.p.*) were injected 3 times a week for 4 weeks.

Table 2. Effects of Na_2SeO_3 on AnuA induction by $HgCl_2$ (II).

$HgCl_2$ (mg/kg)	Na_2SeO_3 (mg/kg)	Positive/Examined	Titer
0	0	0/8	
	0.46	0/8	
	1.84	0/8	
0.25	0	8/8	6.4 ± 1.1
	0.46	8/8	5.9 ± 0.9
1.0	0	8/8	6.0 ± 1.0
	1.84	7/7	5.7 ± 1.0

$HgCl_2$ (0.1 ml/mouse, *s.c.*) and Na_2SeO_3 (0.5 ml/mouse, *i.p.*) were injected in male mice 3 times a week for 4 weeks.

suggested that the pathological mechanism of autoimmunity induction by $HgCl_2$ might be independent of its toxicity. Since doses of $HgCl_2$ necessary to induce AnuA were far less than those to induce toxic effects, it might also be possible that doses of Na_2SeO_3 used in these experiments were too small to inhibit autoimmunity induction by $HgCl_2$.

The possible mechanism(s) of autoimmunity induced by heavy metals and chemicals may include (1) release of autoantigen(s) in the circulation due to their toxic effects; (2) alteration of autoantigen(s) due to their combination with self antigen(s); or (3) direct effects on lymphocytes following activation of helper T cells and subsequent polyclonal activation of B cells[2, 21, 22]. The precise mechanism of AnuA induction by $HgCl_2$ requires further examination.

References

1) Kazantzis G. Hypersensitivity: Clinical aspects. in Dayan AD, Hertel RF, Heseltine E, Kazantzis G, Smith EM, Van der Venne MT eds. Immunotoxicity of metals and immunotoxicology. Plenum Publishing Corporation, New York, 1990; 67–74.
2) Pelletier L, Castedo M, Bellon B, Druet P. Mercury and autoimmunity. in Dean JH, Luster MI, Munson AE, Kimber I eds. Immunotoxicology and immunopharmacology (second edition). Raven Press, New Tork, 1994; 539–52.
3) Weening JJ, Fleuren GJ, Hoedmaeker PhJ. Demonstration of antinuclear antibodies in mercuric chloride- induced glomerulopathy in the rats. Lab Invest 1978; 39: 405–11.
4) Roman-Franco A, Turiello M, Albine B. Ossi E, Milgrom F, Andres GA. Anti-basement membrane antibodies and antigen-antibody complexes in rabbit injected with mercuric chloride. Clin Immunol Immunopathol 1978; 9: 464–81.
5) Robinson CJG, Abraham AA, Balazs T. Induction of antinuclear antibodies by mercuric chloride in mice. Clin Exp Immunol 1984; 58: 300–6.
6) Hultman P, Enestrom S. Mercury induced antinuclear antibodies in mice: Characterization and correlation with renal immune complex deposits. Clin Exp Immunol 1988; 71: 269–74.
7) Reutter R, Tessars G, Vohr HW, Gleichmann E, Luhrmann R. Mercuric chloride induces autoantibodies against U3 small nuclear ribonucleoprotein in susceptible mice. Proc Natl Acad Sci USA 1989; 86: 337–41.
8) Saegusa J, Yamamoto S, Iwai H, Ueda K. Antinucleolar autoantibody induced in mice by mercuric

chloride. Ind Health 1990; 28: 21–30.
9) Pelletier L, Pasquire R, Hirsch F, Sapin C, Rossert J, Druet P. Autoreactive T cells in mercury-induced autoimmune disease: *in vitro* demonstration. J Immunol 1986; 137: 2548–54.
10) Pelletier L, Pasquire R, Rossert J, Vial MC, Mandet C, Druet P. Autoreactive T cells in mercury-induced autoimmunity. Ability to induce the autoimmune disease. J Immunol 1988; 140: 750–4.
11) Hultman P, Enestrom S. Murine mercury-induced immune-complex disease: Effect of cyclophosphamide treatment and importance of T cells. Brit J Exp Pathol 1989; 70: 227–36.
12) Robinson CJG, Balazs T, Egorov IK. Mercuric chloride-, gold sodium thiomate, and d-penicillamine-induced antunuclear antibodies in mice. Toxicol Appl Pharmacol 1986; 86: 159–69.
13) Kolb H, Toyka KV, Gleichmann E. Histocompatibility antigens and chemical reactivity in autoimmunity. Immunol Today 1987; 8: 3–6.
14) Saegusa J, Kiuchi Y, Itoh T. Antinucleolar autoantibody induced in mice by mercuric chloride: Strain difference in susceptibility. Exp Anim 1990; 39: 597–9.
15) Saegusa J, Kubota H, Kiuchi Y. Antinucleolar autoantibody induced in mice by mercuric chloride: A genetic study. Ind Health 1991; 29: 167–70.
16) Atten J, Bosman CB, Rozing J, Stijnen T, Hoedemaeker PhJ, Weening JJ. Mercuric chloride-induced autoimmunity in the Brown Norway rat. Cellular kinetic and major histocompatibility complex antigen expression. Am J Pathol 1988; 133: 127–38.
17) Dubey C, Bellon F, Hirsch F, Kuhn J, Vial MC, Goldman M, Druet P. Increased expression of class II major histocompatibility complexes molecules on B cells in the rats susceptible or resistant to $HgCl_2$-induced autoimmunity. Clin Exp Immunol 1991; 86: 118–23.
18) van Vliet E, Uhrberg M, Stein C, Gleichmann E. MHC control of IL-4-dependent enhancement of B cell Ia expression and Ig class switching in mice treated with mercuric chloride. Int Arch Allergy Immnol 1993; 392–401.
19) Parizek J, Ostadalova I. The protective effect of small amounts of selenite in sublimate intoxication. Experientia 1967; 23: 142–3.
20) Magos L, Webb M. The interaction of selenium with cadmium and mercury. CRC Crit Rev Toxicol 1980; 8: 1–41.
21) Bigazzi PE. Mechanisms of chemical-induced autoimmunity. in Dean JH, Luster MI, Munson AE, Amos H eds. Immnotoxicology and Immunopharmacology Raven press, New York 1985; 277–90.
22) Goldman M, Druet P, Gleichmann E. TH2 cells in systemic autoimmunity: insights from allogenic diseases and chemically induced autoimmunity. Immunol Today 1991; 12: 223–7.

National Institute of Industrial Health,
21-1, Nagao 6-chome, Tama-ku,
Kawasaki 214, Japan

Junzo SAEGUSA and
Hisaya KUBOTA

(Received October 19, 1995 and in revised form December 4, 1995)

Exp. Anim. 44(3), 255–259, 1995

—Note—

Deodorization of Laboratory Animal Facilities by Ozone

Tien Mei PAN[1)*], Kouji SHIMODA[1)], Yi CAI[1)], Yoshihiro KIUCHI[2)], Kazumasa NAKAMA[3)], Toshio AKIMOTO[3)], Yasuaki NAGASHIMA[4)], Masakazu KAI[4)], Michio OHIRA[5)], Junzo SAEGUSA[6)], Takatoshi KUHARA[7)], and Kazuyoshi MAEJIMA[1)]

*[1)]Laboratory Animal Center, Keio University School of Medicine, 35 Shinanomachi, Shinjuku, Tokyo 160, [2)]Yokohama City University School of Medicine, Yokohama, Kanagawa 236, [3)]Nippon Medical School, Bunkyo, Tokyo 113, [4)]Zexel, Inc, Konancho, Saitama, 360-01, [5)]Ebara, Inc, Kawasaki, Kanagawa 211, [6)]National Institute of Industrial Health, Kawasaki, Kanagawa 214, [7)]Teikyo University School of Medicine, Itabashi, Tokyo 173, Japan and *Present address : Guangdong Provincial People's Hospital, Zhungzang Road 2, Gaungzhou, People's Republic of China*

Abstract: *Deodorizing effect of ozone was investigated comparing two types of compact ozonizing apparatus made on an experimental basis. The concentrations of ammonia and trimethylamine were examined as an indicator for deodorizing effect of ozone in animal rooms of rats and guinea pigs at laboratory animal facilities of three different universities. Both of the ozonizing apparatus were able to remove ammonia and trimethylamine in animal rooms, with no significant difference in the performance of the two apparatus.*

Key words: *animal facility, deodorization, ozone*

In order to deodorize our living environment, several methods are available: to remove the source of bad smell, to force smell out by ventilation, to allow materials emitting smell to react with an appropriate substance (degradation), to allow materials emitting smell to bind to an appropriate substance (adsorption), to cover up smell with a competing substance, etc. These methods are used independently or in combination.

The most commonly used method in laboratory animal facilities is adsorption method, i.e., to place adsorbents such as activated charcoal, iron powder and diatomite in cages, trays under the cages or in the corner of animal rooms, which are the main sources of bad smell, or to force room air to pass through adsorbent. These adsorption methods are effective only when a large amount of adsorbent equivalent to substances emitting bad smell is used or adsorbent is frequently renewed.

In general, the amount of substances emitting bad smell in animal facilities is enormous, therefore, it is not economical to use adsorption methods for deodorization of animal facilities. There are several other methods for deodorization of animal facilities, but at present none of them is practical, because they are not so effective in animal facilities where the amount of substances emitting bad smell is great, they cost too

(Received 6 January 1995 / Accepted 2 May 1995)

Address corresponding: Pan Tien Mei, Guangdong Provincial People's Hospital, Zhungzang Road 2, Gaungzhou, People's Republic of China

much, or because may affect physiological conditions of laboratory animals and the results of experiments.

Recently compact systems for deodorization and disinfection of the inside of refrigerators and cars have been put to practical use, in which a small amount of ozone is emitted and recovered. Therefore, the authors have investigated the efficacy of ozone for deodorization of animal facilities during the course of studies on ozone fumigation since 1990 [1–3].

The authors have been performing basic and applied studies on ozone fumigation as one of the new methods for sanitation of animal facilities. The experiments using Bacillus spores led to a conclusion that 2–6 hour ozone fumigation was practically effective in sterilizing materials such as cages, bedding and working clothes, at concentrations of 200–600 ppm under the conditions of room temperature and 90% relative humidity. Toxicity of residual ozone gas on the materials after sterilization was not observed for laboratory animals under the above conditions.

In 1992, Sato *et al.* reported the new system combining ozonizer and catalyst for elimination of bad smell from the animal room [4]. Ammonia elimination rate by this system was 1.4 to 3.2 times as compared with conventional ways using an activated absorber or a water scrubber. For deodorization of the animal facilities, this system seemed to be effective but expensive, because of large scaled equipment.

The authors made a plan to develope compact ozonizing apparatus and to investigate its deodorizing effect. In the present study, the concentrations of substances emitting bad smell were examined in animal facilities of Nippon Medical School, Yokohama City University School of Medicine and Keio University School of Medicine, comparing the two types of ozonizing apparatus made on an experimental basis by Ebara, Inc. (Kawasaki, Japan) and Zexel, Inc. (Saitama, Japan).

The animal facility of Nippon Medical School is equipped with a simplified air-conditioning system which controls room air by using a wall air-conditioner and heater and a ventilating fan; the animal facilities of Yokohama City University and Keio University are equipped with centralized air-conditioning systems which supply 100% fresh air. Any specialized systems were not adopted for daily care of animals, and all the experiments were carried out according to the Guideline for Animal Experimentation (JALAS, 1987).

The ozonizing apparatus made by Zexel, Inc. (hereinafter referred as "Z apparatus") has the ability to process 60 m^3 air per hour with external dimensions of 550 × 750 × 310 mm, and consumes 100 W/100 V electric power, and that made by Ebara, Inc. ("E apparatus") has the ability to process 60 m^3 air per hour with external dimensions of 550 × 750 × 310 mm and consumes 250 W/100 V electric power. The ozonizing mechanisms of both apparatus are similar: they take in room air and allows to react with a small amount of ozone gas which is generated by electric discharge and substances emitting bad smell are degraded by an oxidizing effect of ozone [4]. Immediately thereafter, residual ozone is resolved using a catalyzer, and finally they return ozone-free air devoid of bad smell into the room.

The concentrations of ammonia and trimethylamine in room air were examined using gas-detectors (Gastec, Kohmei-Rikagaku Co., Tokyo, Japan) for each gas as representative substances emitting bad smell in animal facilities [5].

A laboratory animal facility equipped with a simplified air-conditioning system: The Z apparatus was placed in an animal room for conventional guinea pigs housing 90 animals in 60 m^3 at the animal facility of Nippon Medical School, where air is controlled at 21–26°C by an air-conditioner and a 24-hour-operating ventilating fan. The guinea pigs were housed in wire-mesh cages of 35 × 50 × 42 cm in dimensions with 1–5 animal (s) for each cage. Feces and urine were dropped onto trays under the cages, and the trays were changed once every day.

An animal technician usually began working at 9:00 a.m. in the animal room and the routine work was finished before noon. The door of the animal room was always kept closed except when the animal technician was working. The average number of researchers going in and out of the room was 5 per day. A lighting cycle was of 14-hour light and 10-hour darkness (6:00 a.m. : on; 8:00 p.m. : off).

The ozonizing apparatus was operated 6 hours a day (10:00 a.m. to 4:00 p.m.). The concentrations of ammonia and trimethylamine were assessed for six successive days at the two points, i.e., in the center of the animal room and beside the ventilating fan, immediately before starting and after stopping the operation of the apparatus.

Table 1. The concentrations of ammonia and trimethylamine in an animal room for guinea pigs at Nippon Medical School

Substance	Apparatus and its operation	Time	Concentration in ppm: M±SD (n)	t-value
Ammonia	Z : yes	10 a.m.	2.92 ± 0.40 (12)	4.940**
		4 p.m.	1.85 ± 0.40 (12)	
	Z : no	10 a.m.	3.83 ± 1.18 (6)	2.143
		4 p.m.	2.63 ± 0.71 (6)	
Trimethylamine	Z : yes	10 a.m.	2.80 ± 1.22 (12)	2.421*
		4 p.m.	1.88 ± 0.51 (12)	
	Z : no	10 a.m.	4.62 ± 1.66 (6)	1.169
		4 p.m.	3.37 ± 0.71 (6)	

**: Significant at p=0.01. *: Significant at p=0.05. The ozonizing apparatus was set to start operating at 10:00 a.m. and to stop operating at 4:00 p.m. on the same day.

Because there were no significant differences between the days examined and the points where the samples were collected, the mean values and standard deviations were calculated by sample number of 12 (=6 × 2). As shown in Table 1, the mean concentrations of ammonia and trimethylamine were decreased by 37% and 33%, respectively, after operating the ozonizing apparatus for 6 hours: the decrease being statistically significant (ammonia: t=4.940, $p \leqq 0.01$; trimethylamine: t=2.421, $p \leqq 0.05$).

To make sure, similar experiments were carried out for three successive days without operation of the ozonizing apparatus. The concentrations of ammonia and trimethylamine which were detected at 4:00 p.m. were 27–31% lower as compared with those detected at 10:00 a.m., but the differences were not statistically significant (ammonia: t=2.143; trimethylamine: t=1.169).

There was a strong correlation between the concentrations of ammonia and trimethylamine (r=0.96). However, it is not appropriate to detect only one of them as a representative indicator for bad smell in animal rooms, since the generating mechanisms for ammonia and trimethylamine are different.

A laboratiry animal facility whose ventilation system was turned off: In order to investigate deodorizing effect of ozone in an animal facility whose ventilation system was turned off and where personnel were not admitted, the concentrations of ammonia and trimethylamine were assessed in an animal room for conventional rats, 400 animals housing in 100 m^3 at the animal facility of Yokohama City University. The rats were housed in polycarbonate cages of 35 × 30 × 18 cm in dimensions with 2–5 animals for each cage.

An animal technician carried out the routine work in the morning in the animal room. No one had free access to the animal room except the animal technician and the personnel performing the present experiments, and the door of the animal room was always kept closed. Since ventilating openings were all stringently sealed up, the air-conditioning system did not work. Therefore, the room temperature varied greatly between 20 and 28°C. A lighting cycle was of 12-hour light and 12-hour darkness (7:00 a.m. : on; 7:00 p.m. : off).

The two types of ozonizing apparatus, the E apparatus and Z apparatus, were used. The ozonizing apparatus were set to start operating at 10:00 a.m. and to stop operating at 4:00 p.m. as in the animal facility of Nippon Medical School. The concentrations of ammonia and trimethylamine were assessed for five successive days at one point of animal room twice a day, immediately before starting and after stopping the operation of the apparatus.

As shown in Table 2, the ammonia concentration in the animal room for rats was approximately 5–10 times as high as that in an animal room for rats which was equipped with a 24-hour air-conditioning system, with a similar volume and an equivalent number of animals, in the animal facility of Keio University (Table 3). In the animal room of Yokohama University for rats whose ventilating openings were experimentally sealed up, the ammonia and trimethylamine concentrations were so high that it was almost unbearable for the personnel to

Table 2. The concentrations of ammonia and trimethylamine in an animal room for rats at Yokohama City University School of Medicine

Substance	Apparatus and its operation	Time	Concentration in ppm: M±SD (n)	t-value
Ammonia	Z : yes	10 a.m.	11.92 ± 3.87 (5)	2.387*
		4 p.m.	6.86 ± 2.74 (5)	
	E : yes	10 a.m.	11.92 ± 3.24 (5)	2.523*
		4 p.m.	6.96± 2.99 (5)	
Trimethylamine	Z : yes	10 a.m.	11.32 ± 3.47 (5)	2.462*
		4 p.m.	6.38 ± 2.78 (5)	
	E : yes	10 a.m.	11.92 ± 2.81 (5)	2.416*
		4 p.m.	7.16 ± 3.38 (5)	

* : Significant at p=0.05. The ozonizing apparatus were set to start operating at 10:00 a.m. and to stop operating at 4:00 p.m. on the same day.

Table 3. The concentration of ammonia in an animal room for rats at Keio University School of Medicine

Substance	Time	Apparatus and its operation	Concentration in ppm: M±SD (n)	t-value
Ammonia	1–2 a.m.	Z : yes	2.07 ± 0.16 (16)	11.632**
		Z : no	2.86 ± 0.18 (8)	
	0–1 p.m.	Z : yes	0.94 ± 0.05 (16)	6.625**
		Z : no	1.15 ± 0.11 (8)	

** : Significant at p=0.01. The ozonizing apparatus was operated continuously for 4 days after 2 days without operating the apparatus.

stay in the animal room for a long time.

When the ozonizing apparatus were operated for 6 hours, the ammonia and trimethylamine concentrations in this aminal room decreased to 56–60%. The decreases were statistically significant at p=0.05 level (the Z apparatus, ammonia: t=2.387, trimethylamine: t=2.462; the E apparatus, ammonia: t=2.523, trimethylamine: t=2.416). To sum up, both the ozonizing apparatus were able to remove ammonia and trimethylamine in animal room, but there was no significant difference in deodorizing effect between the two types of ozonizing apparatus.

A laboratory animal facility where the ozonizing apparatus was continuously operated: The Z apparatus was placed in an animal room for conventional rats, 350 animals housing in 85 m^3 at the animal facility of Keio University. The rats were housed in wire-mesh cages of 26 × 39 × 119 cm in dimensions with 1–6 animal (s) for each cage. Feces and urine were dropped onto "cascade" under the cages. The cascade was flushed once in every 30 min with 40 *l* water. The room temperature was maintained at 22–24°C by a centralized air-conditioning system. A lighting cycle was of 12-hour light and 12-hour darkness (8:00 a.m. : on; 8:00 p.m. : off).

The concentration of ammonia without operation of the ozonizing apparatus was assessed for two successive days at four different points which were separated at equal intervals in the animal room, twice a day, i.e., 1:00 a.m. to 2:00 a.m. and 12:00 noon to 1:00 p.m. Thereafter, the ozonizing apparatus was operated continuously, and the ammonia concentration was assessed four successive days at four points twice a day.

Because of no differences between the days examined and the points sampled, the mean values and standard deviations were calculated by sample number of 8 (=4 × 2) or 16 (=4 × 4). As shown in Table 3, the ammonia concentration after operation of the ozonizing

apparatus was significantly decreased, as compared with that before operation of the apparatus.

The ammonia concentration detected at daytime (12:00 noon to 1:00 p.m.) was evidently lower than that at midnight (1:00 a.m. to 2:00 a.m.) in both the cases with and without operation of the ozonizing apparatus. In this animal facility, there has been a tendency that bad smell was weaker in the daytime, since animal technicians or researchers opened the door of the animal room which was connected to an experimentation room of 100 m^3 at 8:00 a.m. and usually closed the door at 4:00 p.m.

The substances emitting bad smell might be increased at night due to a lower ventilation rate. The present results indicated that deodorizing effect of ozone in laboratory animal facilities could be improved by increasing the amount of ozone generated and/or by increasing ventilation rate in animal rooms.

References

1. Pan, T. M., Liu, Y. X., Shimoda, K., Maejima, K., Kuhara, T., Urano, T., Ishihara, T., and Kasai, N. 1990. *Exp. Anim.* 39: 371–376.
2. Pan, T. M., Shimoda, K., Maejima, K., Kuhara, T., Saegusa, J., Tsukumi, K., Urano, T., and Nagashima, Y. 1993. *Acta Lab. Anim. Sci. Sinica* 1: 120–127.
3. Pan, T. M., Shimoda, K., Maejima, K., Kuhara, T., Tsukumi, K., and Urano, T. 1992. *Exp. Anim.* 41: 181–187.
4. Sato, L. N., Fujisawa, N., Maeda, Y., and Fukui, M. 1992. *Exp. Anim.* 41: 39–45.
5. Urano, T. 1993. Biomedical Research Mannual. Vol. 1. Methods of Animal Experimentation (Maejima, K. and Nagasawa, H. eds.), pp. 119–122. Yokendo, Tokyo (in Japanese).

Exp. Anim. 45(4), 353–360, 1996

IQI/Jic Mice Have Thymic B Cells

Junzo SAEGUSA, Akinori YASUDA, and Hisayo KUBOTA

Laboratory of Experimental Toxicology, National Institute of Industrial Health, 6–21–1, Nagao, Tama-ku, Kawasaki 214, Japan

Abstract: *The thymus of IQI/Jic mice aged 3 to 15 months was studied chronologically by flow cytometry and immunohistochemistry. Thymic B cells (Thy B) expressing the surface marker $B220^{+}IgM^{+}$ were detected in both sexes, but were more prominent in females. Thy B appeared as early as 4 months of age in female mice, and the incidence of Thy B-positive mice and average Thy B ratio in thymocytes increased with age, reaching over 90% and 15%, respectively, after 9 months of age. In males, Thy B-positive animals appeared around 9 months of age and its incidence and average ratio increased gradually to 53% and 5%, respectively, at 15 months. The Thy B-rich thymus was thickened with cortical atrophy and medullary hyperplasia. Small- to medium-sized Thy B crowded and often formed follicle-like structures in the medulla. When mice of various ages were injected with mercuric chloride to induce antinucleolar antibody, many Thy B-rich animals could not develop the antibody, implying that these animals are immunologically impaired. IQI/Jic can be a novel strain to elucidate the relationship between the presence of Thy B and disorders of the immune system.*

Key words: *B cells, IQI/Jic mouse, thymus*

Introduction

The thymus is the primary site for T lineage differentiation and is responsible for generating T cells. After homing to the thymus, T cell precursors undergo extensive proliferation, and thereafter, interact with various accessory cells associated with positive and negative selection, and ultimately differentiate into functionally competent cells, which migrate to the periphery. But not all lymphocytes present in the normal thymus are T cells: a small proportion are B cells [1, 4, 5, 7, 8].

The thymus in mice reaches its greatest size at sexual maturity [3]. With increasing age, there is a gradual loss of thymic parenchyma which is characterized by progressive thinning of the cortex and lymphocyte depletion, but, unlike humans, complete atrophy never occurs even in old mice [3]. The degree of atrophy varies considerably depending upon individuals and strains.

IQI/Jic is an inbred strain established from ICR mice in Japan [6]. This strain is a high responder to the induction of antinucleolar autoantibody by mercuric chloride [13]. During pathological studies on this strain, we noticed recently that the thymus of aged female mice was as large as that of young mice and had follicle-like structures in the medulla. This observation

(Received 9 April 1996 / Accepted 31 May 1996)

Address corresponding: J. Saegusa, Laboratory of Experimental Toxicology, National Institute of Industrial Health, 6–21–1, Nagao, Tama-ku, Kawasaki 214, Japan

prompted us to study the thymus of IQI/Jic mice. The present paper deals with chronological analyses by flow cytometry and immunohistochemistry.

Materials and Methods

Mice: Specific pathogen free IQI/Jic mice were originally obtained from the Central Institute of Experimental Animals (Kawasaki, Japan), and maintained in the semi-barrier system of our animal facility. The animals were kept in polycarbonate cages and given free access to standard laboratory pellets (CE-2, Clea Japan Ltd., Tokyo, Japan) and tap water. The animal room is air-conditioned (temperature 22 ± 2°C, relative humidity 55 ± 5%) and has a 12 hr light-dark cycle. Mice were confirmed by serological monitoring to be free from any infectious pathogens.

More than 10 mice of both sexes aged 3, 6, 9, 12 and 15 months were examined. In addition, 4- and 5-month-old females were studied. All mice used in this study were clinically healthy and without any gross changes. The mice were anesthetized with chloroform, bled by heart puncture and then the thymus was removed carefully from adjacent lymph nodes avoiding blood contamination. The tissue was cut transversely at the central area and the lower part of both lobes was examined by flow cytometry. The rest of the tissue was used for histopathological and immunohistochemical study.

Antibodies: Monoclonal antibodies to mouse CD4 (clone GK1.5, rat IgG2b) and CD8 (clone 2.43, rat IgG2b) were obtained from Dr. K. Ueda at the Institute of Public Health, Tokyo Japan. Anti-mouse Fc γII/III receptor (clone 2.4G2, rat IgG1) and anti-mouse B220 (clone RA3-6B2, rat IgG2a) with or without conjugation of phycoerythrin (PE) were purchased from Pharmingen, California, USA. PE-conjugated anti-mouse CD4 (clone GK1.5, rat IgG2b) and fluoresceinisothiocyanate (FITC)-conjugated anti-mouse CD8 (clone 53-6.7, rat IgG2a) were purchased from Becton Dickinson, California, USA. FITC-conjugated goat anti-mouse IgM was purchased from Jackson Immunoresearch Laboratory, Pennsylvania, USA. Affinity-purified goat anti-mouse IgM and anti-mouse IgG were purchased from Cappel, Pennsylvania, USA. Biotinylated rabbit anti-rat IgG and anti-goat IgG were purchased from Vector Laboratories, California, USA.

Flow cytometry: Single-cell suspensions were made from the thymus of freshly killed mice in phosphate-buffered saline (PBS) containing 0.05% sodium azide, and analyzed in two-color analysis by FACScan (Becton Dickinson). The cell suspensions were first incubated with anti-mouse Fc γ II/III receptor to prevent non-specific binding of antibodies reacting later. An aliquot of the cell suspensions was then incubated with PE-conjugated anti-mouse B220 and FITC-conjugated goat anti-mouse IgM, or with PE-conjugated anti-mouse CD4 and FITC-conjugated anti-mouse CD8. We considered $B220^+IgM^+$ cells as B cells and mice in which B cells comprised more than 2% of thymocytes were considered thymic B cell (Thy B)-positive animals.

Histopathology: The thymus was fixed in 10% neutral-buffered formalin and embedded in paraffin. Sections cut at a thickness of 4 μm were stained with hematoxylin and eosin.

Immunohistochemistry: The abidin-biotin complex (ABC) method (Vectastain ABC kit, Vector Laboratories) was used. The thymic lobe was embedded and frozen in O.C.T. compound (Miles Laboratories, Indiana, USA). Sections cut at a thickness of 4 μm were dried and treated in acetone for 10 min. Sections were incubated with 10% bovine serum albumin in PBS for 30 min. Serial sections were incubated with monoclonal antibodies to B220, CD4, CD8, and goat anti-mouse IgM, or goat anti-mouse IgG in a refrigerator overnight. After antibody incubation, sections were reacted with biotinylated rabbit anti-rat IgG or anti-goat IgG for 30 min, and then endogenous peroxidase activity was blocked by incubation with a 0.3% H_2O_2 methanol solution for 20 min. Slides were incubated with avidin DH:biotinylated horseradish peroxidase H complex for 60 min and the peroxidase reaction was initiated in a 0.05% solution of diaminobenzidine (Wako Pure Chemicals, Tokyo, Japan) and 0.01% H_2O_2 in PBS. Sections were counterstained with methyl green. All reagent incubations were carried out at room temperature unless otherwise specified.

Anitinucleolar autoantibody induction by mercuric chloride: A stock solution of 10 mg/m*l* of mercuric chloride ($HgCl_2$) (Wako Pure Chemicals) in sterile 0.9% saline was prepared at the beginning of the experiment and aliquots of the stock solutions were diluted with sterile 0.9% saline before injection. Five to 10 mice of both sexes aged 1.5, 5, 9 and 12 months were injected

Table 1. Incidence of Thymic B cell-positive mice at various ages

Sex		Age (Months)						
		3	4	5	6	9	12	15
Male	positive	0			0	6	5	8
	examined	10	ND	ND	24	19	11	15
	(%)	(0)			(0)	(32)	(46)	(53)
Female	positive	0	1	3	11	20	14	19
	examined	13	15	10	28	21	15	20
	(%)	(0)	(7)	(30)	(39)	(95)	(93)	(95)

Thymocytes with B220$^+$IgM$^+$ surface marker were considered thymic B cells (Thy B) and those mice with Thy B comprising more than 2% of thymocytes were considered Thy B-positive. ND: not done.

subcutaneously 1 mg/kg $HgCl_2$ (0.1 ml/mouse) 3 times a week for 4 weeks. Immediately (one day) and 3 months after the final injection, mice were anesthetized in chloroform and then bled by heart puncture. Sera were separated and stored at −20°C until use. The antinucleolar autoantibody (AnuA) levels were determined by indirect immunofluorescence using cultured rat myoid cells as the substrate and FITC-conjugated goat anti-mouse IgG. The sera were diluted with PBS by a 2-fold dilution starting at 1:10. The AnuA titer is expressed as the value for the tube with the highest dilution showing nucleolar staining. Details of the method are described elsewhere [12].

Results

Analysis by flow cytometry: Chronological analyses at an interval of 3 months showed that Thy B-positive mice appeared after 6 and 9 months of age in females and males, respectively (Table 1). Since 11 of 28 female mice aged 6 months were Thy B-positive, we suspect that these mice may begin to appear earlier than at 6 months. Additional study in 4- and 5-month-old females revealed that 1 of 15 and 3 of 10 mice were Thy B-positive, respectively, indicating that Thy B appeared as early as 4 months of age.

The incidence of Thy B-positive mice increased with age. In females, the incidence increased gradually to 39% by 6 months, and suddenly exceeded 90% after 9 months. In males, the incidence increases gradually throughout the observation and reached 53% at 15 months.

The Thy B ratio in thymocytes also increased with age in both sexes, but this tendency was more prominent in females. While it varied considerably among cases, the average ratio of each age group increased gradually, reaching 31% and 5% in females and males, respectively, at 15 months of age (Fig. 1). Female

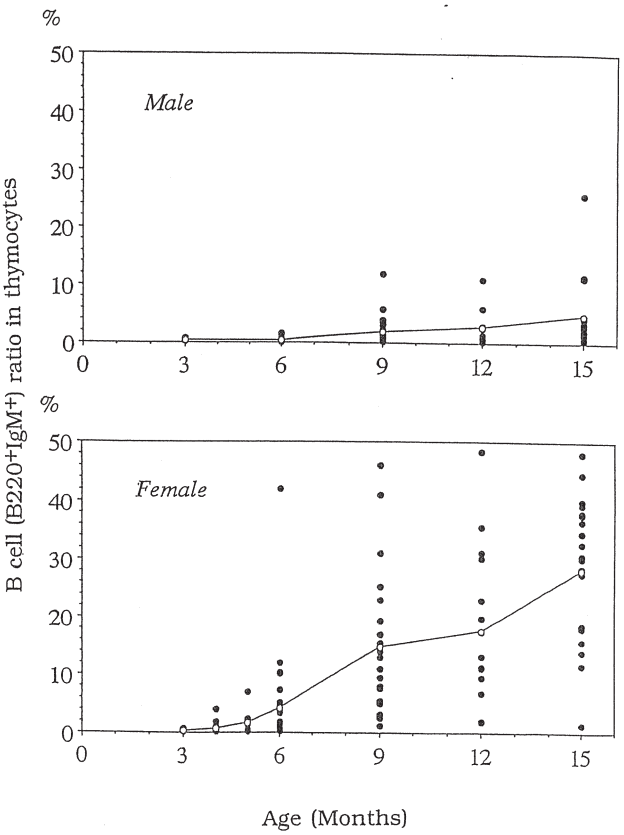

Fig. 1. B cell (B220$^+$IgM$^+$) ratio in thymocytes. Closed circles indicate individual data and open circle shows the mean for each age.

mice having more than 35% Thy B were often found after 9 months and the most prominent cases had about 50% Thy B. On the other hand, only a few male mice older than 9 months had more than 10% Thy B.

The relative ratios of $CD4^+CD8^+$, $CD4^+CD8^-$ and $CD4^-CD8^+$ T cells in thymus having a few Thy B were in normal range (Fig. 2A). However, the relative ratio of immature $CD4^+CD8^+$ T cells decreased and those of mature $CD4^+CD8^-$ and $CD4^-CD8^+$ T cells increased in Thy B-rich thymus (Fig. 2B).

Histopathology and Immunohistochemistry: The Thy B-rich thymus of female mice older than 9 months were as large as those of young mice. The thymus had a thin cortex and hyperplastic medulla where small- to medium-sized lymphocytes crowded and often formed follicle-like structures (Fig. 3A). Germinal centers were less frequently found. Often infiltration of plasma cells with distended cytoplasm and frequent globular eosinophilic inclusions was seen in the atrophic cortex (Fig. 3B). While no gross changes were observed, medullary accumulation of small- to medium-sized lymphocytes was noted in Thy B-positive males.

Immunohistochemical study clearly showed that B cells ($B220^+IgM^+$) consisted of crowded lymphocytes and follicle-like structures in the medulla (Fig. 4). Plasma cells infiltrating into the cortex had IgM or IgG in their cytoplasm. A small number of $CD4^+CD8^+$ T cells consisted of atrophic cortex, and a few $CD4^+$ and rare $CD8^+$ T cells were dispersed in the medulla.

Antinucleolar autoantibody induction by $HgCl_2$: As a preliminary function study, mice of various ages were injected with $HgCl_2$ to induce AnuA. In males, a high

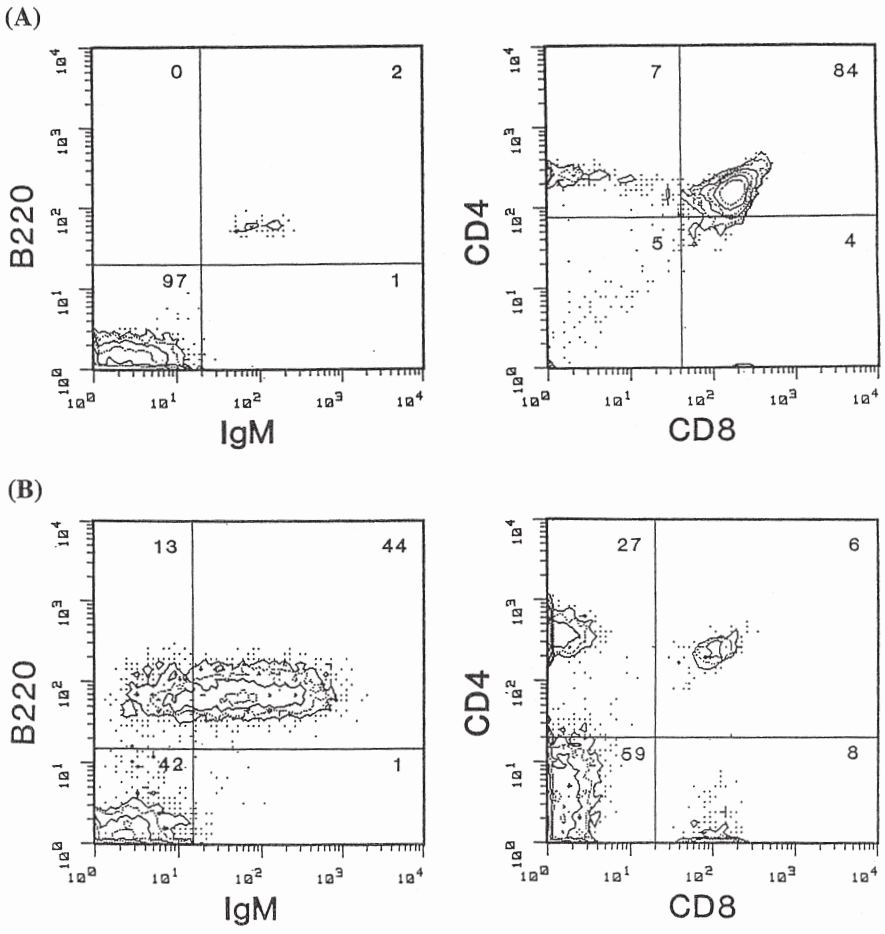

Fig. 2. Analysis of thymocytes from two 15 month-old female mice by flow cytometry. (A) a mouse with 2% thymic B cells, (B) a mouse with 44% thymic B cells. Results are expressed as percentage of total thymocytes (shown in upper right).

titer of AnuA was induced and kept at high levels 3 months after the treatment in all animals except a case of 5-month-old group. Though similar results were obtained in female mice 1.5 months of age, AnuA was not induced or not maintained in some female mice older than 5 months (Table 2). AnuA was induced in only 2 of 6 female mice aged 12 months. Three months after the treatment, AnuA was detected in 1 of 6 and 3

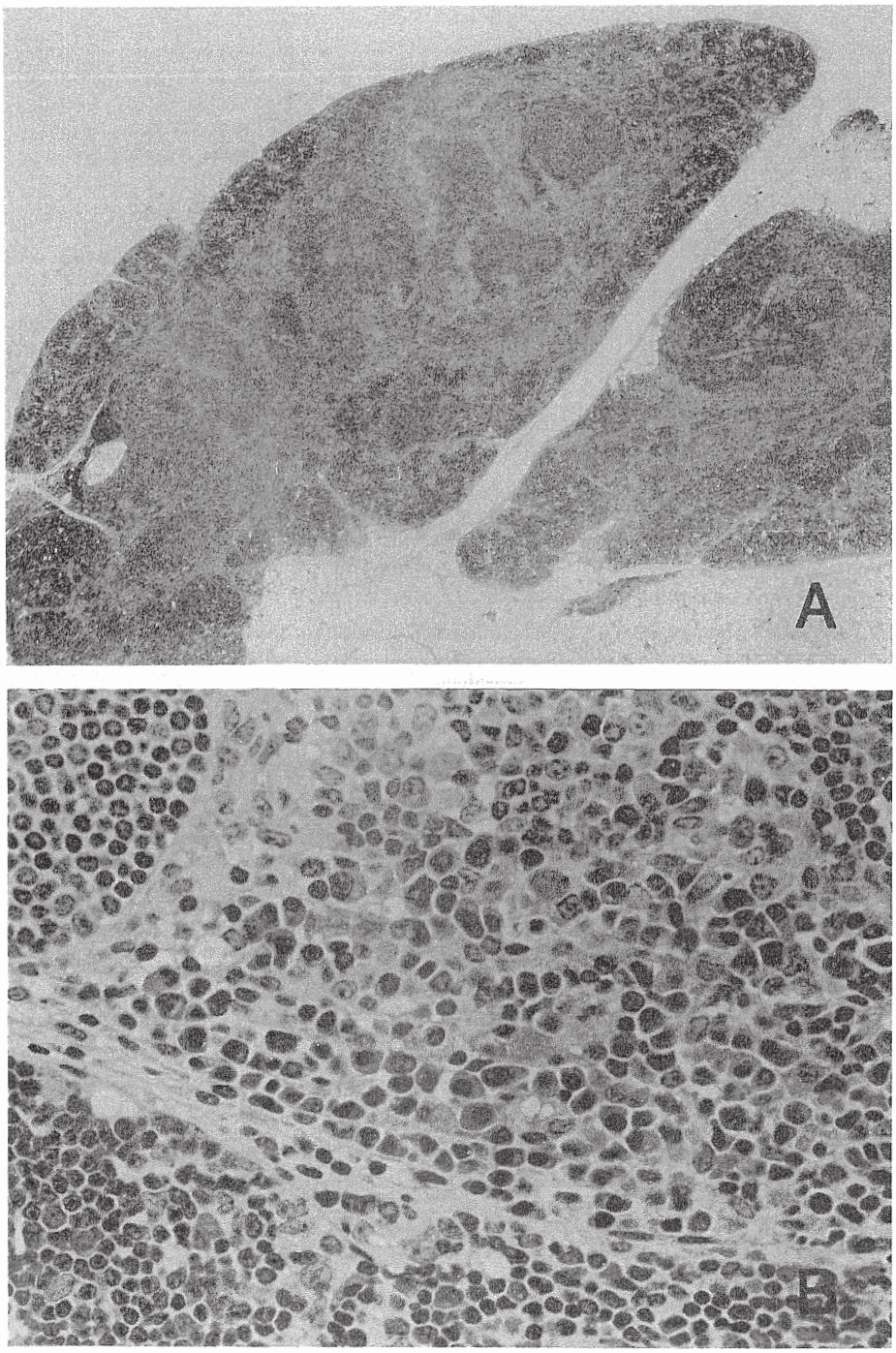

Fig. 3. Thymus of a 12 month-old female mouse. Frequent formation of follicle-like structure in the medulla (A) and plasma cell infiltration in atrophic cortex (B). Hematoxylin and eosin stain.

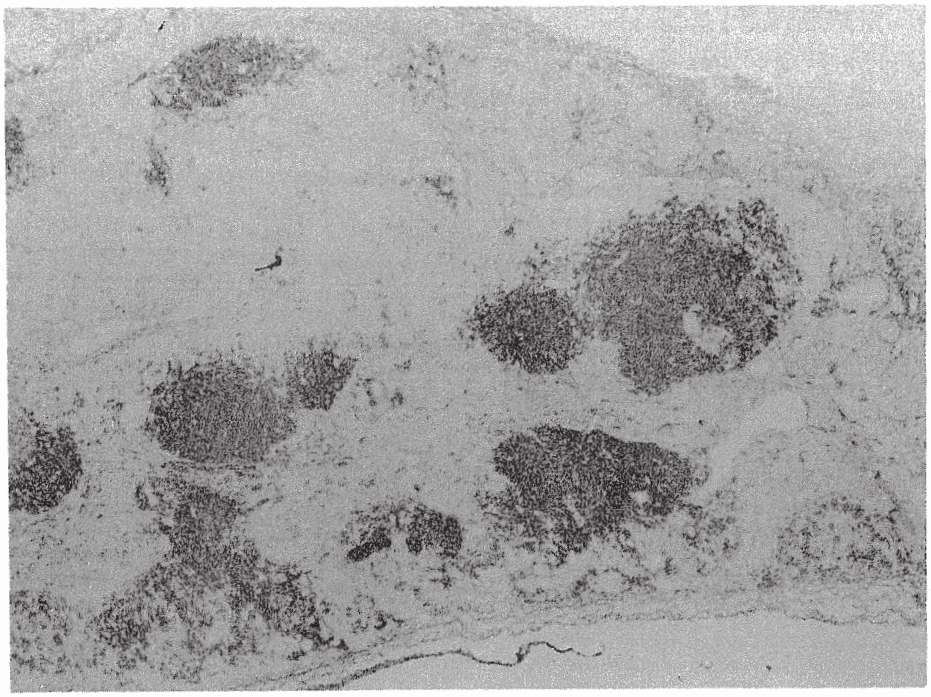

Fig. 4. Cluster of B220$^+$ cells in the medulla of the thymus from a 12-month-old female mouse. Avidin-biotin complex immunoperoxidase stain.

Table 2. Antinucleolar autoantibody induction by mercuric chloride

Sex	Age (months)	immediate		3 months	
		positive/examined	titer	positive/examined	titer
Male	1.5	5/5	8 ± 0	6/6	5 ± 1
	5	5/5	7 ± 1	5/6	7 ± 2
	9	8/8	7 ± 1	10/10	8 ± 2
	12	6/6	7 ± 1	ND	
Female	1.5	5/5	8 ± 1	6/6	7 ± 2
	5	3/5	6 ± 1	1/6	7
	9	6/7	6 ± 2	3/8	6 ± 2
	12	2/6	7 ± 2	ND	

Mice were injected with 1 mg/kg $HgCl_2$ 3 times a week for 4 weeks and bled immediately (one day) and 3 months after the treatment. Antinucleolar autoantibody was determined by indirect immunofluorescence and the titer is expressed as the value of the tube with the highest dilution showing nucleolar staining. ND: not done.

of 8 5- and 9-month-old female mice, respectively. When AnuA was induced, the titer was considerably high immediately and 3 months after the induction, being independent of age and sex.

Although quantitative analysis by flow cytometry was not done, histological and immunohistochemical examination revealed that all AnuA-negative and some AnuA-positive mice had Thy B accumulation in the medulla. The Thy B colonies tended to be more prominent in AnuA-negative mice.

Discussion

The present study clearly showed that IQI/Jic mice

had B cells in the thymic medulla, being more prominent in females. Thy B-positive mice appeared as early as 4 months in females and around 9 months in males. The incidence in females increased gradually to 39% by 6 months, then suddenly reached over 90% after 9 months, and that in males gradually increased and reached 53% at 15 months. The average ratio increased progressively with age, and it reached 31% and 5% in females and males, respectively, at 15 months. These characteristics are very unique, since B lymphocytes are a minor subset (typically 0.2 to 1.0% of total thymocytes) in the thymus of commonly used mouse strains [1, 7].

Histological and immunohistochemical studies indicated that Thy B were located in the medulla where they frequently formed follicle-like structures. Similar lesions were described in aged female ICR mice as lymphoid hyperplasia [3], though the characteristics of hyperplastic lymphoid cells, the incidence of their appearance and its pathological significance are unknown. Since the IQI/Jic mouse strain was established from ICR mice [6] and the pathological change was more frequent and prominent, gene(s) relating to the thymic lesion might be fixed in this strain.

Previous studies indicated that AnuA induction by $HgCl_2$ occurred in a $CD4^+$ T-cell-dependent manner [9, 10, 12]. The present study revealed that Thy B-rich female mice could not develop AnuA by $HgCl_2$, suggesting that the presence of numerous Thy B might be correlated with functional impairment of $CD4^+$ T cells. Though AnuA induced by $HgCl_2$ was persisted at high levels long after the treatment [11, 12], AnuA was not detected in 5 of 6 and 5 of 8 female mice of 5 and 9 months of age group, respectively, 3 months after the induction (Table 2). It is not clear whether these mice could not develop AnuA or whether they might have lost AnuA in 3 months after induction, because AnuA in these mice was not examined immediately after the treatment. However, these AnuA-negative mice may have become Thy B-positive and lost memory function of $CD4^+$ T cells during 3 months of observation, since the proportion of Thy-B positive female mice suddenly increased after 6 months of age (Table 1). Taken together, $CD4^+$ T cells may be defective in both the induction and memory stages of AnuA production in Thy B-rich IQI/Jic mice. On the other hand, several mice with Thy B successfully developed AnuA which remained at high levels for 3 months. These results imply that there may be a critical Thy B ratio in thymocytes above which immunological disorders are likely to occur. The relationship between the amount of Thy B and functional defects in $CD4^+$ T cells is still unclear and its pathological significance needs to be determined.

Lymphoid follicles consisting of B cells in thymus were reported in patients with a variety of human autoimmune diseases including myasthenia gravis, Addison's disease, rheumatoid arthritis, systemic lupus erythematosus, autoimmune thyroiditis and autoimmune hemolytic anemia [4]. In mice, medullary hyperplasia of thymus with cortical atrophy, quite similar to present case, was reported in autoimmune-prone mice such as NZBxW F1, MRL/lpr and BXSB [2]. These studies suggest that formation of lymphoid follicles, which consisted of B cells, in the thymic medulla might be closely related to the onset of autoimmune diseases. In fact, monoclonal antibodies obtained from thymic B cells of myasthenia gravis patients produced various autoantibodies relating the syndrome of the disease [14]. Our ongoing study indicated that female IQI/Jic mice suffered from slowly progressive sialoadenitis similar to human Sjogren's syndrome after 9 months of age (Saegusa *et al.*, submitted for publication). Further pathological studies on intrinsic disease in IQI/Jic mice is in progress.

Regarding this evidence, IQI/Jic mice can be a novel strain to elucidate the relationship between the presence of Thy B and immunological impairment as well as development of autoimmune diseases.

References

1. Andreu-Sanchez, J.L., Faro, J., Alonso, J.M., Paige, C.J., Martinez-A, C., and Marcos, M.A.R. 1990. Ontogenic characterization of thymic B lymphocytes. Analysis in different mouse strains. *Eur. J. Immunol.* 20: 1767–1773.
2. Andrews, B.S., Eisenberg, R.A., Theofilopoulos, A.N., Izui, S., Wilson, C.B., McConahey, P.J., Murphy, E.D., Roth, J.B., and Dixon, F.J. 1978. Spontaneous murine lupus-like syndromes. Clinical and immunopathological manifestations in several strains. *J. exp. Med.* 148: 1198–1215.
3. Faccini, J.M., Abbott, D.P., and Paulus, G.J.J. 1990. Haemato-poietic and lymphatic system. pp. 24–36. *In*: Mouse histopathology-A glossary for use in toxicity and carcinogenicity studies (Faccini, J.M., Abbott, D.P., and Paulus, G.J.J. eds.), Elsevier, Amsterdam.
4. Henry, K. 1992. The thymus gland. pp. 27–140. *In*:

Systemic Pathology (3rd edition) vol. 7, Thymus, lymph nodes, spleen and lymphatics (Henry, K. and Symmers, W.St.C. eds.), Churchill Livingstone, London.

5. Isaccson, G., Norton, A.J., and Addis, B.J. 1987. The human thymus contains a novel population of B lymphocytes. *Lancet* ii: 1488–1491.
6. Katoh, H. 1989. Animal models derived from the ICR mouse for human diseases. *Medical Immunology* 17: 353–361 (in Japanese).
7. Miyama-Inaba, M., Kuma, S.I., Inaba, K., Ogata, H., Iwai, H., Yasumizu, R., Muramatsu, S., Steinman, R.M., and Ikehara, S. 1988. Unusual phenotype of B cells in the thymus of normal mice. *J. exp. Med.* 168: 811–816.
8. Palestra, G., Tridente, G., Botto-Micca, Fl., Novero, D., Valente, G., and Godio, L. 1983. Immunohistochemical and enzyme histochemical contribution to the problem concerning the role of thymus in the pathogenesis of myasthenia gravis. *Virchow Arch (Cell Pathol)* 44: 173–186.
9. Pelletier, L., Pasquier, R., Hirsch, F., Sapin, C., and Druet, P. 1986. Autoreactive T cells in mercury-induced autoimmune disease: *In vitro* demonstration. *J. Immunol.* 137: 2548–2554.
10. Pelletier, L., Pasquier, R., Rossert, J., Vial, M.C., Mandet, C., and Druet, P. 1988. Autoreactive T cells in mercury-induced autoimmune disease: Ability to induce the autoimmune disease. *J. Immunol.* 140: 750–754.
11. Robinson, C.J.G., Abraham, A.A., and Balaz, T. 1984. Induction of antinuclear antibodies by mercuric chloride in mice. *Clin. Exp. Immunol.* 58: 300–306.
12. Saegusa, J., Yamamoto, S., Iwai, H., and Ueda, K. 1990. Antinucleolar autoantibody induced in mice by mercuric chloride. *Ind. Health.* 28: 21–30.
13. Saegusa, J., Kiuchi, Y., and Itoh, T. 1990. Antinucleolar autoantibody induced in mice by mercuric chloride. Strain difference in susceptibility. *Exp. Anim.* 39: 597–599.
14. Williams, C.L. and Lennon, V.A. 1986. Thymic B lymphocyte clone from patients with myasthenia gravis secrete monoclonal striational autoantibodies reacting with myosin, α actinin, or actin. *J. exp. Med.* 164: 1043–1059.

Exp. Anim. 46(2), 103–109, 1997

Correlation of Mast Cells with Spindle Cell Hyperplasia in the Adrenal Cortex of IQI/Jic Mice

Jong-Soo KIM[1, 2)], Hisayo KUBOTA[1)], Kunio DOI[2)], and Junzo SAEGUSA[1)]

[1)]*Laboratory of Experimental Toxicology, National Institute of Industrial Health, 6–21–1 Nagao, Tama-ku, Kawasaki 214, and* [2)]*Department of Veterinary Pathology, Faculty of Agriculture, The University of Tokyo, 1–1–1 Yayoi, Bunkyo-ku, Tokyo 113, Japan*

Abstract: *IQI/Jic mice showed a high incidence of subcapsular spindle cell hyperplasia (SCH) in the adrenal cortex accompanied by prominent mast cell infiltration. SCH-positive animals appeared as early as at 3 months of age, with an incidence of 18% in males and 20% in females. Except for one mouse, all females older than 6 months had the lesion. In males, the incidence increased gradually until 9 months, and was then stable at 75–88% thereafter. The severity of SCH increased with age in both sexes, and the lesions were more prominent in females. Mast cells infiltrated mainly at the sites of spindle cell hyperplasia, and their density was associated with the severity of the lesion. A quantitative morphometric study confirmed a significant correlation between the severity of SCH and the density of mast cells. A histochemical study demonstrated that these mast cells were of the connective tissue-type. These observations indicate that IQI/Jic mice may be a useful strain to elucidate the pathogenesis of SCH in the adrenal cortex in association with mast cell function.*

Key words: *adrenal gland, IQI/Jic mouse, mast cell, spindle cell (type A cell) hyperplasia*

Introduction

Subcapsular cell hyperplasia of the adrenal cortex is common in older mice of many strains, but rarely observed in young mice [8, 12]. Subcapsular cell hyperplasia is of special interest because of its association with the development of adrenocortical tumors [6]. Although spontaneous adrenocortical tumors are rare in mice and limited to old mice of a few inbred strains, gonadectomy usually enhances the development of subcapsular cell hyperplasia in both males and females, and adrenocortical tumors arise frequently in the area of subcapsular cell hyperplasia in such animals [5, 6, 21].

There are two types of subcapsular cell hyperplasia of the adrenal cortex, referred to as "type A cell" and "type B cell" hyperplasia. The type A cells (spindle cells) are usually ovoid, but vary from round to fusiform. The nuclei are round to ovoid and relatively large, and the cytoplasm is scanty and free of lipid. The type B cells (polygonal cells) are polygonal and vary in size, with vacuolated cytoplasm [6, 10].

(Received 5 September 1996 / Accepted 16 October 1996)

Address corresponding: J.-S. Kim, Department of Veterinary Pathology, Faculty of Agriculture, The University of Tokyo, 1–1–1 Yayoi, Bunkyo-ku, Tokyo 113, Japan

IQI/Jic mice are an inbred strain established from the ICR strain in Japan [14]. This strain is a high responder to the induction of antinucleolar autoantibody by mercuric chloride [18]. Aged IQI/Jic mice have thymic B cells [19]. We recently noticed a high incidence of subcapsular spindle cell (type A cell) hyperplasia (SCH) in the adrenal cortex accompanying numerous mast cells in the IQI/Jic strain. This lesion appeared in young animals as well as old animals. In the present study, therefore, we chronologically examined the incidence and pathological severity of SCH, and quantitatively determined the number of mast cells in the adrenal glands of IQI/Jic mice.

Materials and Methods

Animals: IQI/Jic mice maintained in our animal facility, originally obtained from the Central Institute of Experimental Animals (Kawasaki, Japan), were used. The animals were maintained with *ad libitum* access to food (CE-2, Clea, Tokyo, Japan) and tap water in a controlled environment (22 ± 2°C, 55 ± 5% relative humidity, 12/12-hr light/dark cycle). A total of 102 male and 115 female mice, free of clinical signs of disease, were provided for this study. Sixteen to 25 mice of each sex were examined at the age of 3, 6, 9, 12 and 15 months, respectively.

Histopathological examination: Mice were anesthetized with chloroform and then bled by heart puncture. Both adrenal glands were taken from each animal and fixed in 10% neutral buffered formalin, routinely processed, and embedded in paraffin. Four-μm thick sections were stained with hematoxylin-eosin or with 0.1% toluidine blue (pH 7.0). The severity of SCH of the adrenal glands was graded as follows: (0) no change; (1) changes involving the focal area (slight); (2) changes involving <25% of the cortex (moderate); (3) changes involving >25% of the cortex (severe). The histopathologic score (0–3) of SCH was recorded for each animal.

Morphometric study: The number of mast cells located in the adrenal parenchyma was counted under a light microscope (× 400) on toluidine blue stained sections. Mast cells located in the adrenal capsules were not counted. The area of the adrenal gland was determined with a computerized image analysis system (LUZEX, NIRECO, Japan). The mast cell counts were expressed as the number of cells/mm^2.

Histochemistry of mast cells: Serial tissue sections were stained for 1 hr with a freshly prepared mixed solution of alcian blue-safranin (0.5% alcian blue and 0.5% safranin, in 0.5N HCl, pH 1.0) or were reacted with a heparin-binding fluorescent dye, berberine sulfate [3, 7]. They were examined with a light or epifluorescent microscope, respectively.

Statistical analyses: Differences between males and females in the density of mast cells were examined by Mann-Whitney U test (two-tailed). Differences between males and females in the incidence of SCH were examined by Fisher's exact test. Correlations between mast cell densities and SCH scores were determined by Spearman's rank correlation coefficient. Probability <0.05 was defined as significant.

Results

Proliferations of spindle cells (type A cells), which were oval to fusiform and had long ovoid nuclei and small amounts of basophilic cytoplasm, were observed beneath the capsule of the adrenal glands (Fig. 1A). The spindle cells were proliferated in the *zona glomerulosa* and occasionally extended downward for various distances into the deep layer of the adrenal cortex. The SCH lesions were focal in mild cases and became diffuse in severe cases. No feature of compression of adjacent tissue nor penetration into the capsule was observed. Mast cells were noted in SCH lesions of the adrenal cortex but were not detected in the medulla (Fig. 1B).

Compared with the males, the females had a higher SCH incidence and severer SCH lesions in the same age groups from 3 to 15 months old. The incidence of SCH was 18% in males and 20% in females at 3 months, and increased with age in both sexes. SCH was significantly more frequent in females than males at 6, 9 and 15 months, but no significant difference was found at 3 or 12 months (Fig. 2). Except for one mouse at 6 months, all female mice older than 6 months showed SCH lesions.

The severity of SCH increased with age in both sexes, and was more prominent in females than males at the same age. In the females, >90% of the mice older than 9 months had moderate to severe lesions, while neither a moderate nor severe lesion was observed at 3 months. In the males, all mice younger than 6 months had slight

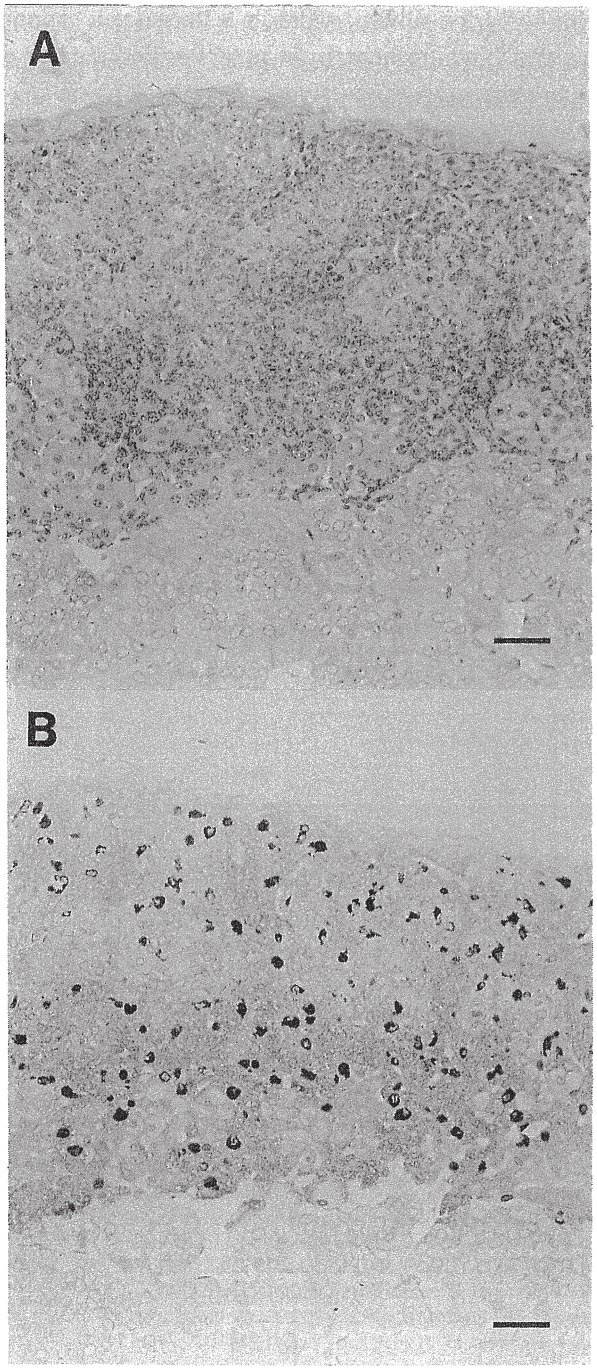

Fig. 1. Adrenal gland of a 12-month-old female IQI/Jic mouse. (A) Diffuse subcapsular spindle cell (type A cell) hyperplasia without compression of parenchyma. HE stain; bar=30 μm. (B) Numerous mast cells are present in the adrenal cortex of a SCH-positive mouse. Toluidine blue stain; bar=30 μm.

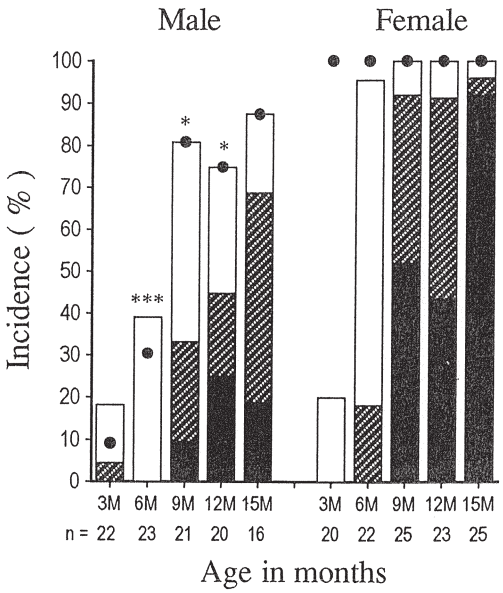

Fig. 2. Incidence of SCH (*bar graph*) and mast cell infiltration (*closed circle*) in the adrenal glands of IQI/Jic mice. n: Number of mice examined. Severity of SCH: slight (□), moderate (▨), severe (■); see text. The incidence of SCH was significantly different from age-matched females (*p<0.05, ***p<0.001)

lesions with one exception, a moderate lesion at 3 months.

Mast cell infiltration was noted in SCH lesions in most of the animals, except for a few male mice younger than 6 months. The more the severity of SCH advanced, the more mast cells infiltrated. To obtain direct evidence of the participation of mast cells in SCH, we quantified the numbers of mast cells in the adrenal glands. The mast cell counts increased greatly with age in both sexes. The mean mast cell density of the adrenal glands was significantly greater in females than males at 3, 6, 9 and 15 months of age (Fig. 3). A significant correlation between the histopathologic score of SCH and the density of mast cells was observed in females older than 6 months and in males older than 9 months (Fig. 4). These findings indicate that mast cells may be closely related to the severity of the SCH.

To determine the histochemical characteristics of the mast cells, we selected tissue sections from females that had high mast cell counts in the adrenal glands, and examined the staining properties of the mast cells with alcian blue-safranin. We also stained the cells

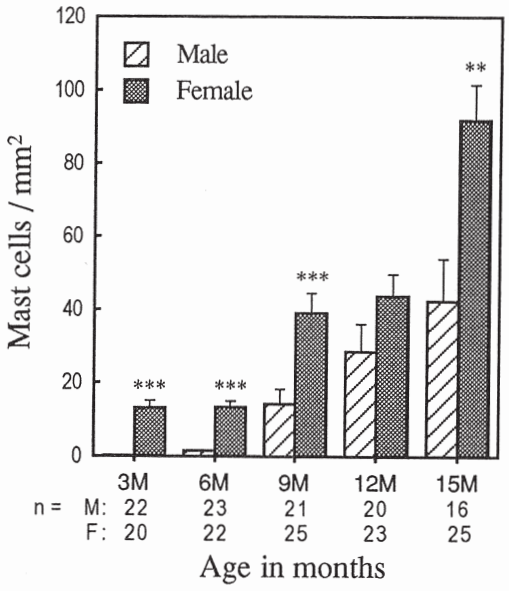

with berberine sulfate, which is a fluorescent cationic dye that binds to heparin in cytoplasmic granules of mature connective tissue-type mast cells (Fig. 5).

The majority (70%) of adrenal gland mast cells from the 3-month-old mice had only alcian blue-positive

Fig. 3. Mast cell density in the adrenal glands of IQI/Jic mice. The more the severity of SCH increased with age, the more mast cells infiltrated. Data are expressed as the mean ± SEM. n: Number of mice examined. Significantly greater than age-matched males (**p<0.01, ***p<0.001).

Fig. 4. Correlation between the severity of SCH and the density of mast cells in the adrenal glands of IQI/Jic mice. See text for severity of SCH. rs: Spearman's rank correlation coefficient. NS: Not significant (p>0.05). n: Number of positive mice with SCH or mast cell infiltration.

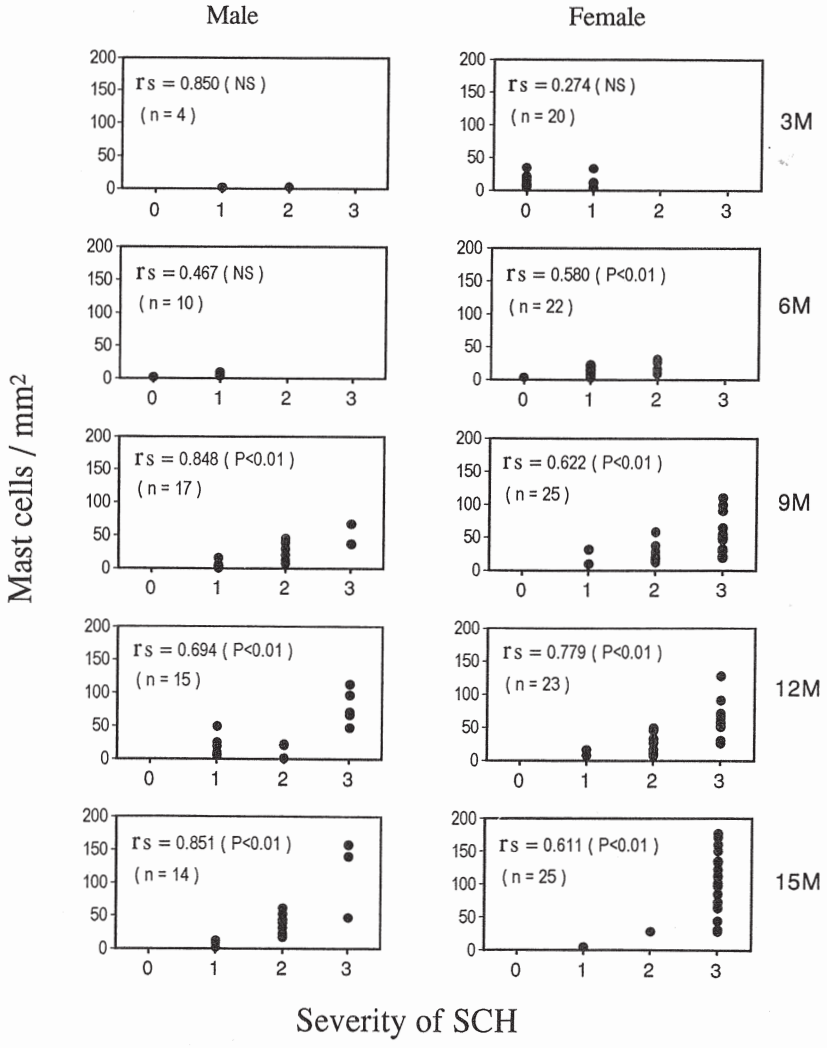

granules and did not show positive staining for safranin. In contrast, a large portion (>60%) of the mast cells from mice older than 6 months had both alcian blue-positive granules and safranin-positive granules (Fig. 6). Mast cells with safranin-positive granules exhibited cytoplasmic reactivity with berberine sulfate.

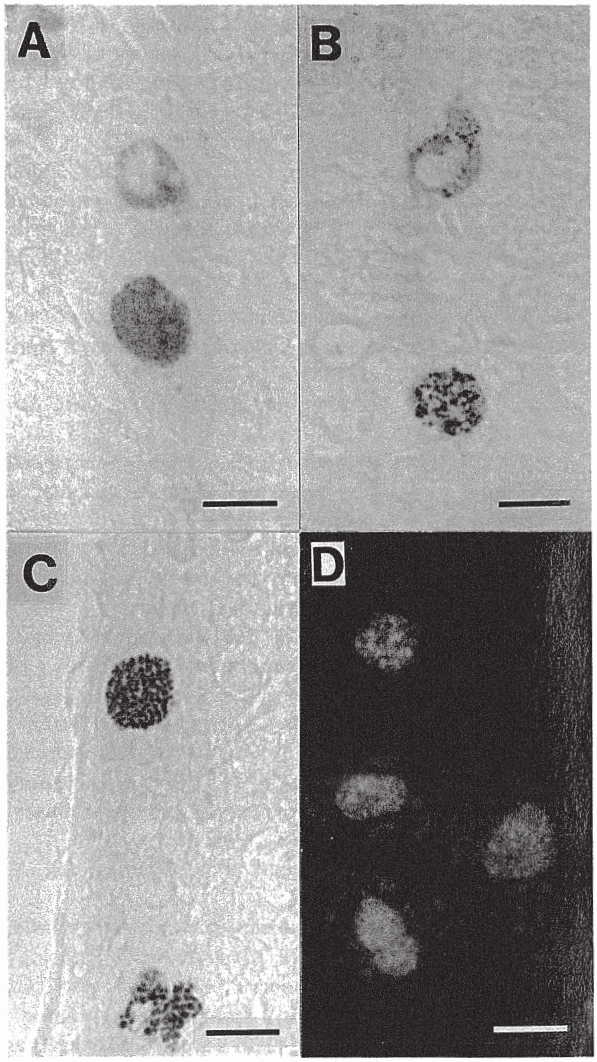

Fig. 5. Histochemical characteristics of mast cells observed in the adrenal glands of IQI/Jic mice. Mast cells from the same mouse showed different staining properties. Alcian blue/safranin staining (A, B, C) and berberine sulfate staining (D). Mast cells containing (A) only alcian blue positive granules, (B) both alcian blue-positive granules and safranin-positive granules, and (C) only safranin-positive granules. (D) Mast cells that contain safranin-positive granules show signs of a cytoplasmic reaction with berberine sulfate. A bright yellowish fluorescence is emitted from the granules. bar=10 μm.

Discussion

The results of the present study demonstrated that IQI/Jic mice had a high incidence of spindle cell (type A cell) hyperplasia in the adrenal cortex accompanying numerous mast cells in the lesions. The chronological examination demonstrated that this strain of mice develops SCH as early as 3 months of age. As far as we know, SCH in such young animals has not been previously reported. This mouse strain may be unique in this respect. The incidence of SCH and its severity increased with age, and the tendency was more prominent in females. These features are similar to those of other strains [10, 12].

The most striking finding of the present study was the presence of a large number of mast cells in the SCH lesions. No association of numerous mast cells with SCH has been reported, but a few mast cells were

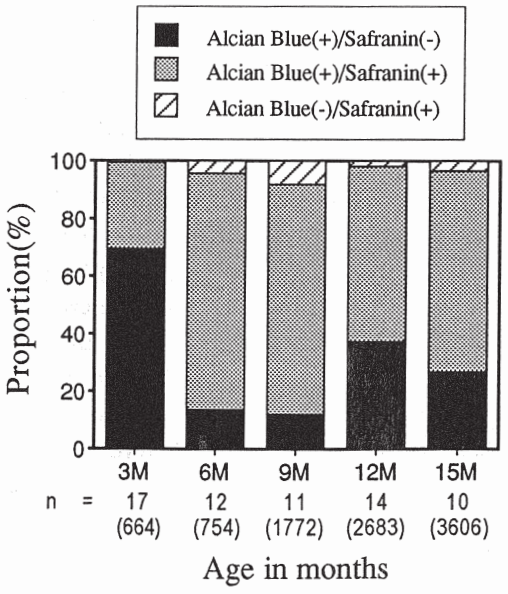

Fig. 6. Distribution of mast cell subpopulations observed in the adrenal glands of female IQI/Jic mice that were stained differently with alcian blue/safranin. The majority of mast cells from 3-month-old mice were safranin-negative immature cells. In contrast, the majority of mast cells from mice older than 6 months were safranin-positive mature cells. n : Number of mice examined. In parentheses, number of mast cells examined.

seen in adrenocortical tumors [9]. Our quantitative morphometric analysis showed a significant correlation between the density of mast cells and the severity of SCH. The abnormal location of a large number of mast cells may therefore be closely associated with the development of SCH. It is possible that mast cells promote the severity of SCH in the adrenal cortex by releasing cytokines such as tumor necrosis factor-α and heparin binding growth factors which were found to have potent angiogenic and mitogenic effects [11, 13, 16, 17].

Two types of mast cells, mucosal and connective tissue types, were initially described in rodents based on the ability of their secretory granules to bind cationic dyes after fixation. Either Carnoy's solution or fixatives containing no more than 0.8% formaldehyde are required for staining mucosal mast cell granules with methylene blue, toluidine blue, or alcian blue [2, 4, 20]. The mast cells in SCH are considered to be of the connective tissue-type because their cytoplasmic granules exhibited metachromasia after fixation with 10% neutral buffered formalin and toluidine blue (pH 7.0) staining, and they contained safranin-positive granules exclusively found in connective tissue-type mast cells when stained with alcian blue/safranin.

The majority of adrenal gland mast cells from the 3-month-old mice were immature cells, since their cytoplasmic granules were stained only with alcian blue and not with safranin [1, 15]. In contrast, the majority of mast cells from mice older than 6 months were mature cells, since they had safranin-positive granules and they exhibited cytoplasmic reactivity with berberine sulfate, suggesting that these cells contain heparin proteoglycan in granules [3, 7]. Most of the mast cells from the 3-month-old mice were therefore less mature in their appearance than those from mice older than 6 months.

We found that IQI/Jic mice had a high incidence and early onset of SCH in the adrenal cortex accompanying prominent mast cell infiltration. In addition, the density of mast cells was significantly correlated with the severity of SCH lesions. These findings indicate that this mouse strain would be useful to use in elucidating the pathogenesis of spindle cell hyperplasia in the adrenal cortex in association with mast cell function.

References

1. Combs, J.W., Lagunoff, D., and Benditt, E.P. 1965. Differentiation and proliferation of embryonic mast cells of the rat. *J. Cell Biol.* 25: 577–592.
2. Crowle, P.K. and Phillips, D.E. 1983. Characteristics of mast cells in Chediak-Higashi mice: Light and electron microscopic studies of connective tissue and mucosal mast cells. *Expl. Cell Biol.* 51: 130–139.
3. Dimlich, R.V.W., Meineke, H.A., Reilly, F.D., and McCuskey, R.S. 1980. The fluorescent staining of heparin in mast cells using berberine sulfate: compatibility with paraformaldehyde or o-phthalaldehyde induced fluorescence and metachromasia. *Stain Technol.* 55: 217–223.
4. Du, T., Friend, D.S., Austen, K.F., and Katz, H.R. 1995. Tissue-dependent differences in the asynchronous appearance of mast cells in normal mice and in congenic mast cell-deficient mice after infusion of normal bone marrow cells. *Clin. Exp. Immunol.* 103: 316–321.
5. Dunn, T.B. 1970. Normal and pathologic anatomy of the adrenal gland of the mouse, including neoplasms. *J. Natl. Cancer Inst.* 44: 1323–1389.
6. Dunn, T.B. 1979. Tumors of the adrenal gland. *IARC Sci. Publ.* 23: 475–485.
7. Enerbäck, L. 1974. Berberine sulphate binding to mast cell polyanions: A cytofluorometric method for the quantitation of heparin. *Histochemistry* 42: 301–313.
8. Faccini, J.M., Abbott, D.P., and Paulus, G.J.J. 1990. Mouse Histopathology—A glossary for use in toxicity and carcinogenicity studies. Elsevier, Amsterdam.
9. Frith, C.H. 1983. Adenoma and carcinoma, adrenal cortex, mouse. pp. 49–56. *In*: Monographs on Pathology of Laboratory Animals—Endocrine System (Jones, T.C., Mohr, U., and Hunt, R.D. eds.), Springer-Verlag, Berlin.
10. Frith, C.H. and Dunn, T.B. 1994. Tumors of the adrenal gland. pp. 595–609. *In*: Pathology of Tumors in Laboratory Animals. Vol. II, Tumors of the mouse, 2nd Ed., (Turusov, V.S. and Mohr, U. eds.), IARC, Lyon.
11. Galli, S.J. 1993. New concepts about the mast cell. *N. Engl. J. Med.* 328: 257–265.
12. Goodmann, D.G. 1983. Subcapsular-cell hyperplasia, adrenal, mouse. pp. 66–68. *In*: Monographs on Pathology of Laboratory Animals—Endocrine System (Jones, T.C., Mohr, U., and Hunt, R.D. eds.), Springer-Verlag, Berlin.
13. Gordon, J.R., Burd, P.R., and Galli S.J. 1990. Mast cells as a source of multifunctional cytokines. *Immunol. Today* 11: 458–464.
14. Katoh, H. 1989. Animal models derived from the ICR for human diseases. *Medical Immunology* 17: 353–361 (in Japanese).
15. Pretlow, T.G. and Cassady I.M. 1970. Separation of mast cells in successive stages of differentiation using programmed gradient sedimentation. *Am. J. Pathol.* 61: 323–339.
16. Qu, Z., Liebler, J.M., Powers, M.R., Galey, T., Ahmadi, P., Huang, X.N., Ansel, J.C., Butterfield, J.H., Planck, S.R., and Rosenbaum, J.T. 1995. Mast cells are a major source

of basic fibroblast growth factor in chronic inflammation and cutaneous hemangioma. *Am. J. Pathol.* 147: 564–573.
17. Reed, J.A., Albino, A.P., and McNutt, A.S. 1995. Human cutaneous mast cells express basic fibroblast growth factor. *Lab. Invest.* 72: 215–222.
18. Saegusa, J., Kiuchi, Y., and Itoh, T. 1990. Antinucleolar autoantibody induced in mice by mercuric chloride. Strain difference in susceptibility. *Exp. Anim.* 39: 597–599.
19. Saegusa, J., Yasuda, A., and Kubota, H. 1996. IQI/Jic mice have thymic B cells. *Exp. Anim.* 45: 353–360.
20. Wingren, U. and Enerbäck, L. 1983. Mucosal mast cells of the rat intestine: A re-evaluation of fixation and staining properties, with special reference to protein blocking and solubility of the granular glycosaminoglycan. *Histochemical J.* 15: 571–582.
21. Woolley, G.W. 1950. Experimental endocrine tumors with special reference to the adrenal cortex. *Recent Prog. Horm. Res.* 5: 383–405.

Exp. Anim. 46(4), 303–306, 1997

—Note—

Subcapsular Cell Hyperplasia and Mast Cell Infiltration in the Adrenal Cortex of Mice: Comparative Study in 7 Inbred Strains

Jong-Soo KIM[1,3], Hisayo KUBOTA[1], Yoshihiro KIUCHI[2], Kunio DOI[3], and Junzo SAEGUSA[1]

[1]*Laboratory of Experimental Toxicology, National Institute of Industrial Health, 6–21–1 Nagao, Tama-ku, Kawasaki 214,* [2]*Laboratory Animal Facility, School of Medicine, Yokohama City University, 3–9 Fukuura, Kanazawa-ku, Yokohama 236, and* [3]*Department of Veterinary Pathology, Faculty of Agriculture, The University of Tokyo, 1–1–1 Yayoi, Bunkyo-ku, Tokyo 113, Japan*

Abstract: *Subcapsular cell hyperplasia (SCH) in the adrenal cortex of aged mice (13–15 months old) was frequent in both sexes of BALB/c, C3H/He, DBA/2J and IQI/Jic mice and in the females of A/J and C57BL/6, although the incidence and severity of SCH were considerably different among mouse strains. Mast cells were closely associated with SCH in the A/J, BALB/c, C57BL/6, DBA/2J and IQI/Jic mice, but not in the C3H/He strain. Compared with other strains, IQI/Jic mice had a significantly larger number of mast cells in the adrenal glands. Our findings suggest that mast cells may participate in the development of SCH, and IQI/Jic would be suitable for studying the pathogenesis of SCH and the role of mast cells in this lesion.*

Key words: *adrenal gland, mast cell, subcapsular cell hyperplasia*

Subcapsular cell hyperplasia (SCH) in the adrenal cortex is commonly observed in older mice of many strains [3, 5]. In some strains, gonadectomy enhances the development of SCH, but the etiology of SCH is not known [1, 2, 7]. Mast cells have been found to play important roles in a variety of physiological, immunological and pathological processes [4]. Our previous study showed a marked increase in mast cells in SCH lesions in the adrenal cortex of IQI/Jic mice [6]. Moreover, a significant correlation between the severity of SCH and the density of mast cells was confirmed [6]. These results suggest that mast cells may be involved in the pathogenesis of SCH in the adrenal cortex of mouse. In the present study, we examined the strain differences in the incidence of SCH and the participation of mast cells in the lesion by using seven inbred mouse strains.

Male and female mice of the A/J, BALB/c, C3H/He, C57BL/6, DBA/2J, IQI/Jic and WHT/Ht strains, aged 13 to 15 months, were studied. IQI/Jic and DBA/2J mice were maintained in the Laboratory Animal Facility of the National Institute of Industrial Health. A/J,

(Received 9 January 1997 / Accepted 19 March 1997)

Address corresponding: J.-S. Kim, Department of Veterinary Pathology, Faculty of Agriculture, The University of Tokyo, 1–1–1 Yayoi, Bunkyo-ku, Tokyo 113, Japan

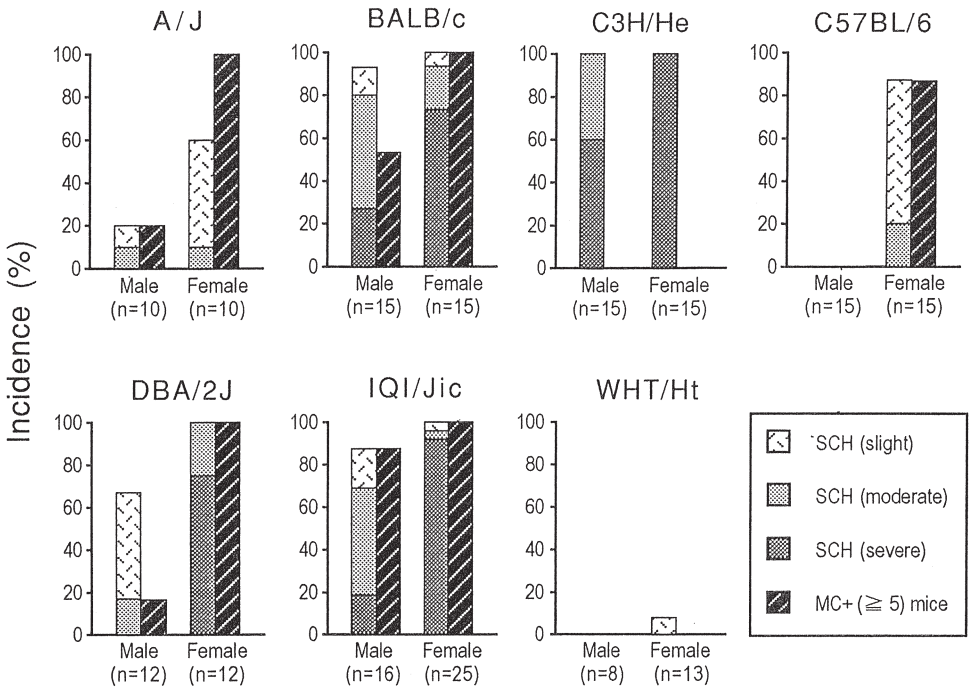

Fig. 1. The incidence of mice with SCH or with mast cell infiltration (MC; ≧5) in the adrenal glands. n: Number of mice examined.

BALB/c, C3H/He, C57BL/6 and WHT/Ht mice were obtained from the Laboratory Animal Facility, School of Medicine, Yokohama City University.

Mice were killed by heart puncture under chloroform anesthesia. Adrenal glands were fixed in 10% neutral buffered formalin, and embedded in paraffin. Tissue sections were stained with hematoxylin-eosin and the pathological severity of the SCH lesion was graded as light, moderate or severe as described previously [6]. Mast cells were identified in sections stained with toluidine blue or alcian blue/safranin, and a mouse with more than 5 mast cells in tissue sections from both adrenal glands was considered to be a mast cell-positive animal. The number of mast cells/mm^2 in the adrenal gland was determined by an image analysis system as described previously [6]. Possible differences between sexes and strains with respect to the incidence of SCH were examined by Fisher's exact test. Comparisons of the density of mast cells among strains and sexes were done by Fisher's post-hoc least significant difference test. Probability <0.05 was defined as significant.

Figure 1 shows the incidence and severity of SCH, and the frequency of animals positive for mast cells in the adrenal glands. SCH was observed in all strains examined, although the incidence and severity of the lesion was considerably different among the mouse strains. SCH was frequent in BALB/c, C3H/He, DBA/2J and IQI/Jic mice of both sexes, and in females of A/J and C57BL/6, but male C57BL/6 mice and all WHT/Ht mice, except for one female, did not show signs of a SCH lesion. The time of SCH-development in these mice may be considerably later than that in other strains examined, since we could find SCH in these strains older than 30 months (data not shown). The order of severity of the SCH lesion in males was: C3H/He > BALB/c ≒ IQI/Jic > DBA/2J ≒ A/J, and that in females was: C3H/He ≒ IQI/Jic ≒ DBA/2J ≒ BALB/c > C57BL/6 ≒ A/J > WHT/Ht. Females had severer SCH lesions than males in all strains examined. Sex difference in the incidence of SCH was most prominent in C57BL/6 mice.

Significant strain differences were found in the participation of mast cells in SCH. Mast cell infiltration was closely associated with the SCH in both sexes of A/J, BALB/c, DBA/2J and IQI/Jic mice and in females

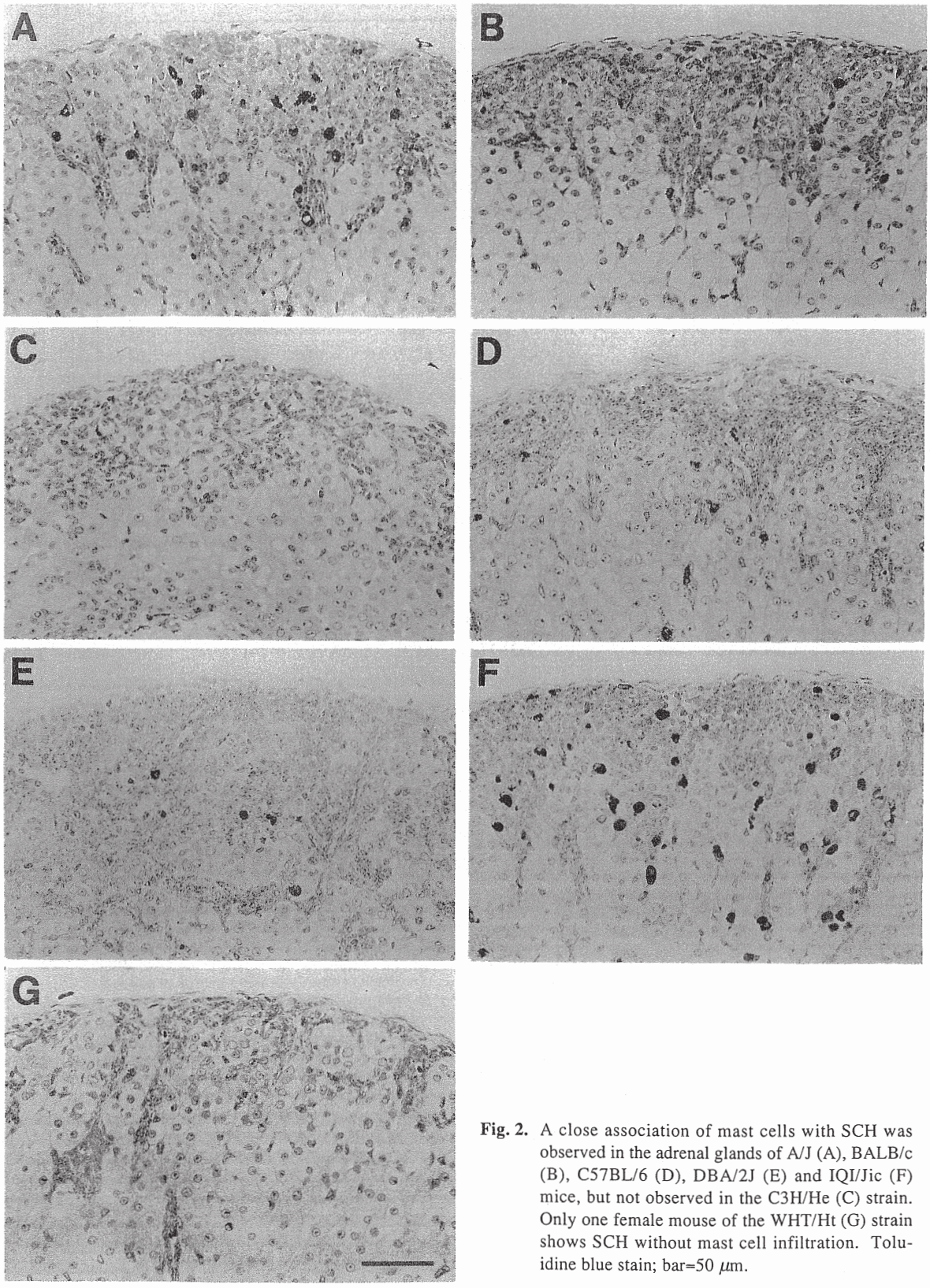

Fig. 2. A close association of mast cells with SCH was observed in the adrenal glands of A/J (A), BALB/c (B), C57BL/6 (D), DBA/2J (E) and IQI/Jic (F) mice, but not observed in the C3H/He (C) strain. Only one female mouse of the WHT/Ht (G) strain shows SCH without mast cell infiltration. Toluidine blue stain; bar=50 μm.

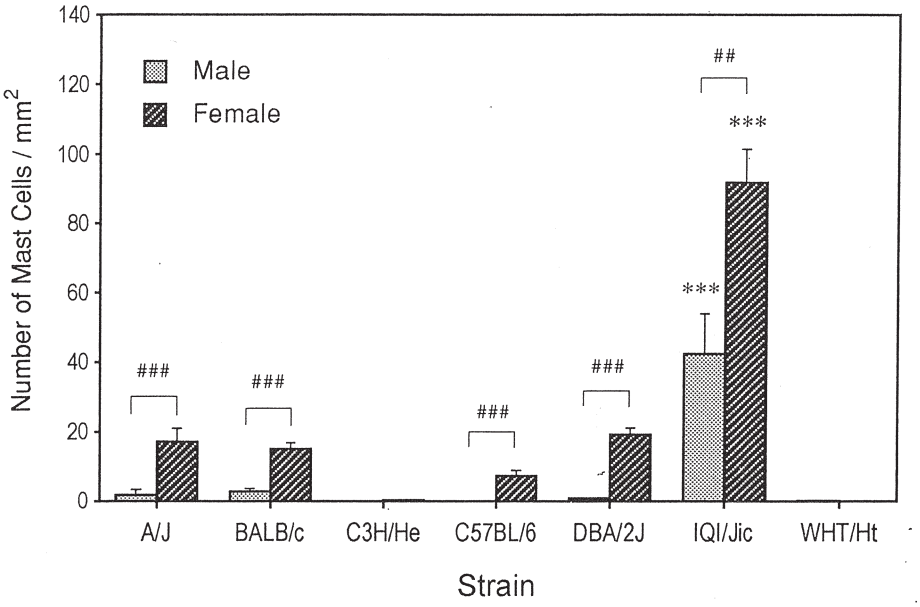

Fig. 3. The density of mast cells in the adrenal glands of mice. Data are the mean ± SEM. Significantly greater than other sex-matched strains (***$p<0.001$) and males (##$p<0.01$, ###$p<0.001$).

of the C57BL/6 mice (Figs. 1 and 2). In the C3H/He strain, however, no mast cell infiltration was observed, although this strain showed a high incidence of SCH with severe lesions. The reason for the difference in the association of mast cells with SCH between C3H/He and other strains is not clear. In the WHT/Ht strain, because only one female mouse was SCH-positive, a meaningful assessment for the association of mast cells with SCH could not be made.

The mean mast cell density in the adrenal gland of IQI/Jic mice was significantly greater (>15 fold in males, $p<0.001$; >5 fold in females, $p<0.001$) than that of sex-matched A/J, BALB/c, C3H/He, C57BL/6, DBA/2J or WHT/Ht mice, respectively (Fig. 3), but no significant differences were seen among the other sex-matched strains excluding the IQI/Jic strain. Females had a greater density of mast cells than males, and significant sex differences were observed in the A/J, BALB/c, C57BL/6, DBA/2J and IQI/Jic mice.

The present study confirms that SCH is not rare in aged mice of various strains, although the severity of SCH is considerably different among mouse strains and between males and females. Our observations further indicate that mast cells are closely associated with the SCH lesion in the adrenal cortex of mice. In addition, IQI/Jic mice, with a higher incidence of SCH and greater density of mast cells than other strains, would be useful for studying the pathogenesis of SCH and the role of mast cells in this lesion.

References

1. Dunn, T.B. 1970. *J. Natl. Cancer Inst.* 44: 1323–1389.
2. Dunn, T.B. 1979. *IARC Sci. Publ.* 23: 475–485.
3. Faccini, J.M., Abbott, D.P., and Paulus, G.J.J. 1990. Mouse Histopathology—A glossary for use in toxicity and carcinogenicity studies, Elsevier, Amsterdam.
4. Galli, S.J. 1993. *N. Engl. J. Med.* 328: 257–265.
5. Goodmann, D.G. 1983. *In*: Monographs on Pathology of Laboratory Animals—Endocrine System (Jones, T.C., Mohr, U., and Hunt, R.D. eds.), Springer-Verlag, Berlin.
6. Kim, J.S., Kubota, H., Doi, K., and Saegusa, J. 1997. *Exp. Anim.* 46: 103–109.
7. Woolley, G.W. 1950. *Recent Prog. Horm. Res.* 5: 383–405.

Sialadenitis in IQI/Jic Mice: A New Animal Model of Sjögren's Syndrome

Junzo SAEGUSA and Hisayo KUBOTA

Laboratory of Experimental Toxicology, National Institute of Industrial Health, 6–21–1 Nagao, Tama-ku, Kawasaki 214, Japan

(Received 17 April 1997/Accepted 12 June 1997)

ABSTRACT. Focal infiltration of lymphocytes with parenchymal destruction was noted in both salivary and lacrimal glands of IQI/Jic mice. The sialadenitis was found in more than 80% of female mice at all ages examined. The lesion progressed after 6 months and became more prominent with age. In contrast, male mice had slight and stable salivary lesions independent of age, though the incidence increased with age. Infiltrating lymphocytes consisted of both T and B cells. The dominant lymphocytes in small foci were $CD4^+$ cells, but the majority of infiltrating cells were B cells ($B220^+$), followed by $CD4^+$ T cells in larger lesions. The ductual epithelium in the foci aberrantly expressed MHC class II antigen. Eight of 24 15-month-old female mice with sialadenitis produced speckled-type IgG antinuclear autoantibody. These findings are similar to those in patients with Sjögren's syndrome. IQI/Jic mice could be a novel animal model of Sjögren's syndrome. — KEY WORDS: animal model, IQI/Jic, sialadenitis, Sjögren's syndrome.

J. Vet. Med. Sci. 59(10): 897–903, 1997

Sjögren's syndrome (SS) is a chronic autoimmune disease characterized by lymphocyte infiltration of the lacrimal and salivary glands, resulting in dry eyes (keratoconjunctivitis sicca) and dry mouth (xerostomia) [3, 21, 26]. The disease may exist as a primary condition or as a secondary condition in association with other autoimmune diseases such as rheumatoid arthritis, systemic lupus erythematosus or systemic sclerosis. It usually appears in women in their fourth and fifth decades in all races, with a female-to-male ratio of 9 to 1 [3, 26]. The lesion remains confined to salivary and lacrimal glands in the majority of the primary SS cases; however, B-cell lymphoma appears in some patients several years after onset [3, 21, 26].

Animal models resembling the human disease are helpful to clarify the important immune mechanism leading to exocrinopathy and development of tissue pathology. Spontaneous and experimental animal models of SS have been presented [4–6, 9, 10, 12, 16, 22, 25, 29, 31], but many models failed to produce the long-lasting lesions seen in human patients.

IQI/Jic is an inbred strain established from ICR mice in Japan [20]. This strain is a high responder to induce antinucleolar autoantibody by mercuric chloride [27]. Recently, we found that aged female mice of this strain had numerous B cells in their thymus [28]. During pathological studies on this strain, we often noticed focal accumulation of mononuclear cells in salivary glands of females. We started, therefore, chronological study on salivary and lacrimal glands in this strain. We found focal lymphocyte infiltration with parenchymal destruction in both organs. The sialadenitis progressed with age and was more prominent in females. These results suggest that this mouse strain could be a novel animal model of SS.

MATERIALS AND METHODS

Mice: Specific pathogen free IQI/Jic mice were originally obtained from the Central Institute of Experimental Animals (Kawasaki, Japan) and maintained in the semi-barrier system of our animal facility. Four week old female BALB/c mice were purchased from CLEA Japan Ltd. (Tokyo, Japan). The animals were kept in polycarbonate cages and were given free access of standard laboratory pellets (CE-2, CLEA Japan Ltd., Tokyo, Japan) and tap water. The animal room was air-conditioned (temperature 22 ± 2°C, relative humidity 55 ± 5%) with a 12-hr light-dark cycle. Serological monitoring revealed that the animals used in this study were free from any infectious pathogens.

Histopathology: Both male and female IQI/Jic mice aged 3, 6, 9, 12 and 15 month and in good general condition were examined. In addition, 7- and 8-month-old females were examined. The mice were anesthetized with chloroform, bled by heart puncture and then autopsied completely. Tissues were fixed in 10% neutral-buffered formalin and embedded in paraffin. Sections cut at a thickness of 4 μm were stained with hematoxylin and eosin, and selected ones were also stained with periodic acid-Schiff, trichromatic or silver stains.

Longitudinal sections at central part of the mandibular glands were prepared and the severity of the lesions was scored as follows. Each inflammatory focus was graded by the number of infiltrating cells (IF) and focus points (FP); 1 FP=foci with less than 20 IF, 2 FP= foci with 20 to 200 IF and 3 FP=foci with more than 201 IF. The total FPs of tissue sections of left and right mandibular glands were calculated, and the severity of the mandibular lesion was evaluated as follows: slight=less than 15 FPs, moderate=16 to 40 FPs and severe=more than 41 FPs.

Antibodies: Monoclonal antibodies (mAbs) to murine CD4 (clone GK1.5, rat IgG2b) and murine CD8 (clone 2.43, rat IgG2b) were obtained from Dr. S. Yamamoto at the Institute of Public Study (Tokyo, Japan). mAb to major histocompatibility complex (MHC) class II antigens, which reacts with $I\text{-}A^{b,d,q}$ and $I\text{-}E^{d,k}$ (clone M5/114.15.2, rat IgG2b), was supplied from Dr. S. Kyuwa at the Institute of Medical Science, the University of Tokyo (Tokyo, Japan). mAb to

murine B220 (clone RA3-6B2, rat IgG2a) with and without conjugation of phycoerythrin (PE), anti-mouse Fc γ II/III receptor (clone 2.4G2, rat IgG1) and biotinylated anti-mouse CD3 (clone 145–2C11, hamster IgG) were purchased from Pharmingen, California U.S.A. PE-conjugated anti-mouse CD4 (clone GK1.5, rat IgG2b), fluorescein-isothiocyanate (FITC)-conjugated anti-mouse CD8 (clone 53–6.7, rat IgG2a) and avidin-conjugated FITC were purchased from Becton Dickinson (California, U.S.A.). mAb to murine Mac-1 antigen (CD11b/CD18) (clone M1/70, rat IgG2b) was purchased from Boehringer-Mannheim (Tokyo, Japan). FITC-conjugated goat sera against mouse IgM or mouse IgG were purchased from Cappel (Pennsylvania, U.S.A.).

Immunohistology: Mandibular gland from 12- and 15-month-old female mice was examined by the avidin-biotin immuno-peroxidase method using the Vectastain ABC kit (Vector Laboratories, California, U.S.A.) to characterize infiltrating mononuclear cells. Mandibular tissue was embedded and frozen in O.C.T. compound (Miles Inc., Indiana, U.S.A.). Serial sections cut at a thickness of 4 μm were incubated with mAbs to CD4, CD8, B220, Mac-1 and class II MHC in a refrigerator overnight. After antibody incubation, sections were incubated with biotinylated rabbit anti-rat IgG (Vector Laboratories) for 30 min and endogenous peroxidase activity was blocked by incubation with 0.3% H_2O_2 methanol solution for 30 min. Then, slides were incubated with avidin DH: biotinylated horseradish peroxidase H complex for 60 min and the peroxidase reaction was initiated in a solution of 0.05% diaminobenzidine (Wako Pure Chemicals, Tokyo, Japan) and 0.01% H_2O_2 in PBS. Sections were counterstained with methyl green. All reagent incubations were carried out at room temperature unless otherwise specified.

Flow cytometric analysis: To verify the results of immunohistology, lymphocytes from the mandibular gland from 12-month-old female mice were analyzed in two-color analysis by FACScan (Becton Dickinson). Single cell suspensions of lymphocytes were made from the mandibular gland of freshly killed mice in PBS containing 0.05% sodium azide, and were first incubated with anti-mouse Fc γ II/III receptor for 30 min to prevent non-specific binding of antibodies reacting later. After washing in PBS, an aliquot of the cell suspensions was incubated with biotinylated anti-mouse CD3 and PE-conjugated anti-mouse B220 for 30 min, washed with cold PBS, and then incubated with avidin-conjugated FITC for 30 min. Other suspensions were incubated with PE-conjugated anti-mouse CD4 and FITC-conjugated anti-mouse CD8 for 30 min. After washing with cold PBS, cell suspensions were applied to FACScan and 10,000 events were aquired from each sample. All reagent incubations were carried out on ice.

Autoantibodies: Mouse sera from 15-month-old mice were stored at -20°C until use. Antinuclear antibody and anti-salivary gland antibody were examined by indirect immunofluorescence using FITC-conjugated goat anti-mouse IgM or anti-mouse IgG. Sera diluted 1:10 with PBS were screened for their reactivity to nuclear antigens using rat myoid cell line as substrate. Positive sera were further examined for their reactivity to SS-A and SS-B antigens prepared from human liver cell line (Hep-2) by double immunodiffusion using ENA-2 kit (MBL Ltd., Nagoya, Japan). Anti-salivary gland antibody was examined by indirect immuno-fluorescence using frozen tissue sections of normal salivary gland from 4-week-old female IQI/Jic and BALB/c mice.

RESULTS

Histopathology: There was focal accumulation of mononuclear cells in the salivary and lacrimal glands, while no gross abnormalities were noted. The infiltrates were prominent around the interlobular ducts in the central portion of the lobule (Fig. 1A). The acini and ducts were extensively replaced by these infiltrates in severe cases, but fibrosis was rare. Destruction of acinar cells and plasma cell infiltration were frequently seen at the periphery of large foci (Fig. 1B). These changes were prominent in the mandibular and extraorbital lacrimal gland (Fig. 1C). Similar lesions were often seen in the parotid gland (Fig. 1D); however, those in the sublingual and infraorbital lacrimal glands were rare.

Sialadenitis was found in more than 80% of female mice at all ages examined, and the severity increased with age (Table 1). Although only slight lesions were observed in most females younger than 6 months, severe lesions suddenly appeared in 10 of 25 (40%) 9-month-old female mice. Thus we studied an additional 10 females of 7 and 8 months of age. Two and 3 mice 7- and 8-month-old, respectively, suffered from severe lesions. These results indicated that the lesion of the female mice might be progressive after 6 months. In contrast, male mice had slight and stable salivary lesions independent of age, though the incidence increased with age (Table 1).

In addition to the lesions in the salivary and lacrimal glands, no specific lesions could be found in either male or female mice younger than 6 months. Systemic lymphadenopathy with plasmacytosis was apparent in female mice with severe sialadenitis. Lymphoid hyperplasia of the thymic medulla was frequent, and segmental glomerular sclerosis and necrotizing vasculitis involving small- to medium-sized arteries were not uncommon in females older than 9 months. However, these extraglandular lesions were not always correlated with the severity of the sialadenitis.

Immunohistology: The infiltrating lymphocytes in salivary lesions consisted of B cells ($B220^+$) and T cells ($CD4^+$ and $CD8^+$). The dominant lymphocytes in small foci were $CD4^+$ cells. However, the majority of infiltrating cells were B cells ($B220^+$), followed by $CD4^+$ cells in larger lesions (Fig. 2). A few $CD8^+$ and Mac-1^+ subsets were scattered in the foci (Fig. 2C). MHC class II antigen was expressed on most infiltrating mononuclear cells and on the ductual epithelial cells in the foci (Fig. 2D).

Flow cytometric analysis: Two color analysis of

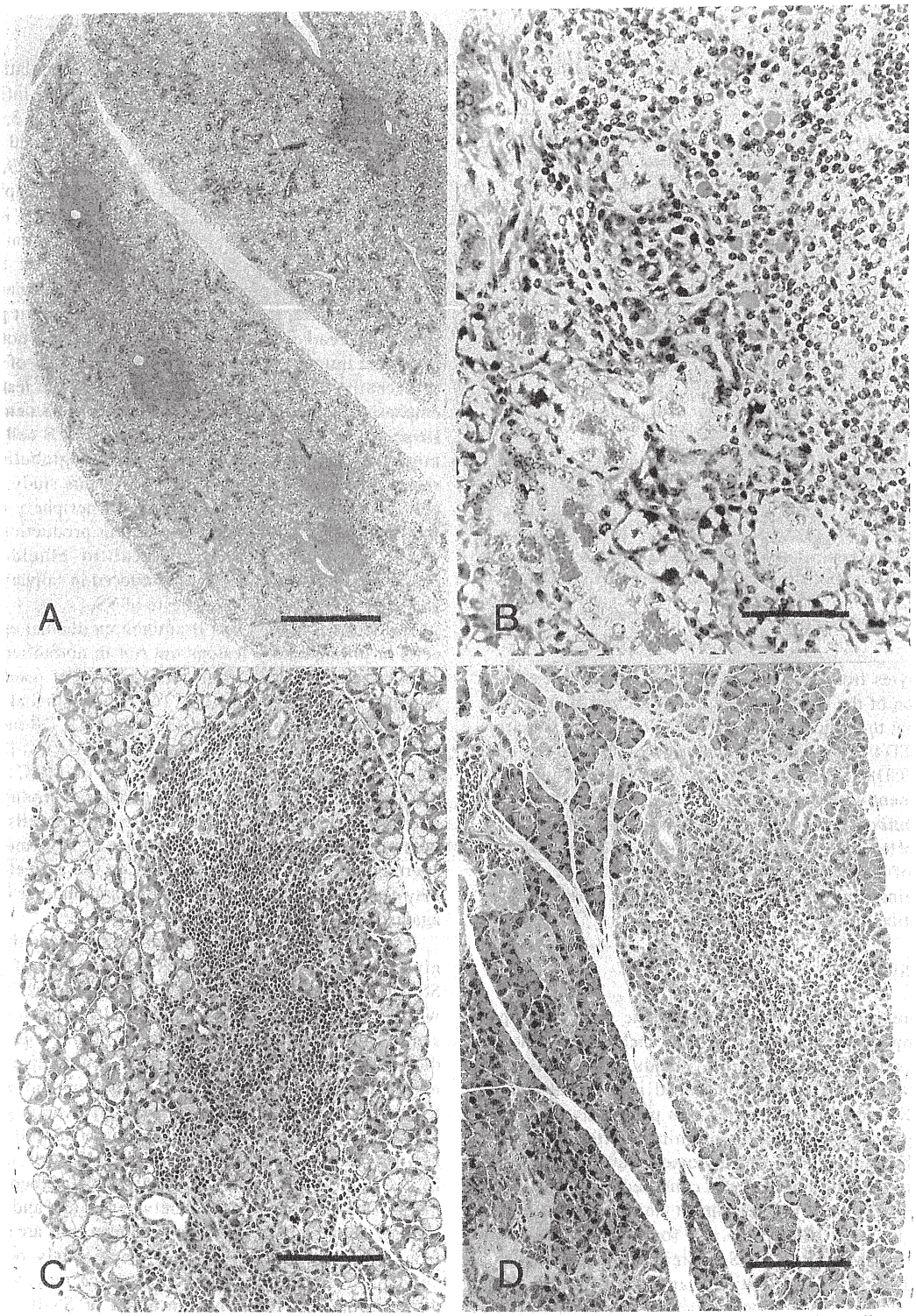

Fig. 1. Sialadenitis in a 12 month-old female IQI/Jic mouse. (A) Multiple focal infiltration of mononuclear cells around interlobular ducts in mandibular gland (Bar=500 μm). (B) Infiltration of lymphocytes and destruction of acini and granulated ducts in mandibular gland. Note infiltration of plasma cells at periphery of the lesion (Bar=50 μm). (C) Infiltration of lymphocytes replacing the aciner cells in extraorbital lacrimal gland (Bar=100 μm). (D) Lymphocyte infiltration in parotid gland (Bar=100 μm). Hematoxylin and eosin stain.

Table 1. Incidence and severity of submandibular adenitis in IQI/Jic mice

Sex	Age (months)	positive/examined (%)	No. of cases with the lesion[a)] Slight	Moderate	Severe
female	3	16/17 (94)	16	0	0
	6	20/25 (80)	19	1	0
	7	9/10 (90)	4	3	2
	8	10/10 (100)	4	3	3
	9	24/25 (96)	6	8	10
	12	30/31 (97)	8	6	16
	15	24/24 (100)	1	7	16
male	3	2/15 (13)	2	0	0
	6	13/23 (57)	13	0	0
	9	14/21 (67)	10	4	0
	12	15/18 (83)	12	3	0
	15	22/23 (96)	18	4	0

a) Each focus was graded by the number of infiltrating cells (IF) and focus point (FP). 1 FP=foci with less than 20 IF, 2 FP=foci with 21 to 200 IF, and 3 FP=foci with more than 201 IF. The total FPs of the lesion from both sides are calculated and the severity of the lesion is evaluated by the total FPs of tissue sections from both sides. Slight=less than 15 FPs, moderate=16 to 40 FPs, and severe=more than 41 FPs.

lymphocytes from the salivary gland revealed that a large population of the infiltrating lymphocytes was B cells (Fig. 3) and that the ratio of B ($B220^+$)/T ($CD3^+$) cells was from 1 to 2. $CD4^+$ cells were dominant in T cells, and the ratio of $CD4^+/CD8^+$ cells was from 5 to 10. These results were in agreement with the immunohistological observations.

Autoantibodies: Speckled-type antinuclear IgG antibody was detected in 8 of 24 females and 1 of 23 males at 15 months of age, but no positive reaction to SS-A or SS-B was obtained by double immunodiffusion. Anti-salivary gland antibody was not detected.

DISCUSSION

The present study showed that IQI/Jic mice developed focal lymphocytic infiltration with parenchymal destruction in both salivary and lacrimal glands. The glandular inflammation was more pronounced in females than in males. Sialadenitis in females was progressive with age and long-lasting, becoming prominent after 9 months. Immunohistological and flow cytometric analyses revealed that the infiltrating lymphocytes consisted of both T and B cells, and $CD4^+$ cells were dominant among T lymphocytes. The ductual epithelium in the foci showed aberrant expression of MHC class II. Some mice with the sialadenitis produced speckled-type antinuclear antibody. Mice with prominent lesions developed systemic lymphoadenopathy with plasmacytosis, suggesting hypergamma-globulinemia. These syndrome observed in IQI/Jic mice fulfil the basic features of SS [3, 21, 26], indicating that this mouse strain could be a novel animal model of SS.

Immunohistological study of lymphocyte subsets indicated that $CD4^+$ cells were the major population in T lymphocytes. This result is in agreement with infiltrating cells in small salivary glands of SS patients [2, 3, 13, 21, 24, 26, 28, 32]. Similar observations were reported in other mouse models of SS [4, 6-10, 14, 16, 18, 19, 25, 29, 31]. It also revealed that the dominant infiltrating lymphocytes were T cells in small foci, but those were B cells in larger lesions. This observation suggested a progression from T cell-dominant foci with later accumulation of B cells. Similar results were reported in the studies on human SS [1, 13, 24], therefore, this mouse strain might make it possible to study the early events and the identification of potentially important immune reactions in the pathogenesis of SS.

Recently, examination of the B cells in the lesion was emphasized [11, 17, 23]. Salivary glands in SS patients are suspected to be a major site of activation of B cells which might secrete large amounts of immunoglobulins with rheumatoid factor activity [11, 17]. In this study, plasma cell infiltration was often found at the periphery of large foci, indicating active immunoglobulin production. This strain, therefore, may be useful to elucidate the characteristics of autoantibodies produced in salivary glands and their roles in the pathogenesis of SS.

We detected MHC class II antigen on ductual epithelial cells in inflammatory lesions but not in normal epithelial cells of salivary gland in this study. Similar results were obtained in MRL/lpr mice [12, 16, 19]. Epithelial cells of salivary glands from SS patients express HLA DR molecules whereas those of normal salivary glands do not [21, 24]. The induction of aberrant expression of MHC class II molecules is suspected to be due to local production of interferon γ by T cells [15, 24]. Since $CD4^+$ T cells interact with peptide antigen presented by class II MHC molecules, aberrant induction of this molecule on the epithelial cells may cause $CD4^+$ T cells to generate an autoimmune response against the epithelium.

It is well known that antinuclear antibody which usually give a speckled pattern is present in 40 to 50% of primary SS patients [3, 21, 26]. Speckled-type antinuclear antibody was detected in 33% of 15-month-old female mice with sialadenitis in the present study. However, this autoantibody did not react with SS-A or SS-B antigens prepared from human liver cell line Hep-2. Since the immuno-diffusion techniques were not sensitive enough [10], we might have failed to detect the autoantibody. St Clair *et al.* [30] reported anti-La autoantibody production in MRL/lpr mice by ELISA, although the pattern of recognition of recombinant human La antigen differed between mice and human patients, suggesting the epitopes on human cells are different from those on murine cells. Spontaneously occurring antinuclear autoantibody in IQI/Jic mice may recognize different epitopes from human SS-A or SS-B antigens; therefore, murine nuclear antigens should be prepared to identify the antigen of antinuclear autoantibody produced in this mouse. Anti-salivary gland autoantibody was not detected in this study, while its production was reported in aged mice with sialadenitis [7–9]. Organ-specific

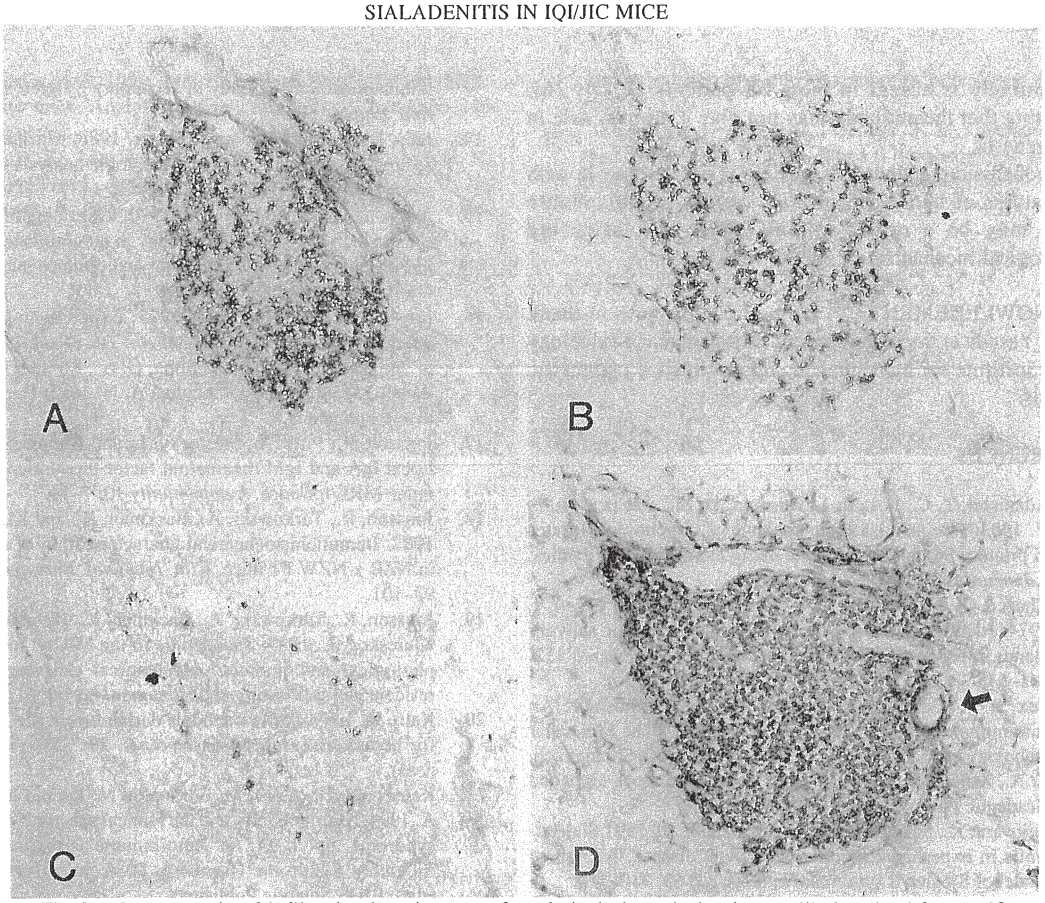

Fig. 2. Immunostain of infiltrating lymphocytes of a relatively large lesion in mandibular gland from a 12 month-old female mice. (A) B220+ (B) lymphocytes, (B) CD4+ lymphocytes and (C) CD8+ lymphocytes. (D) Expression of MHC class II antigen. Most infiltrating cells and interstitial dendritic cells are positive. Ductal epithelial cells (arrow) in the lesion aberrantly express the MHC class II antigen. ABC stain.

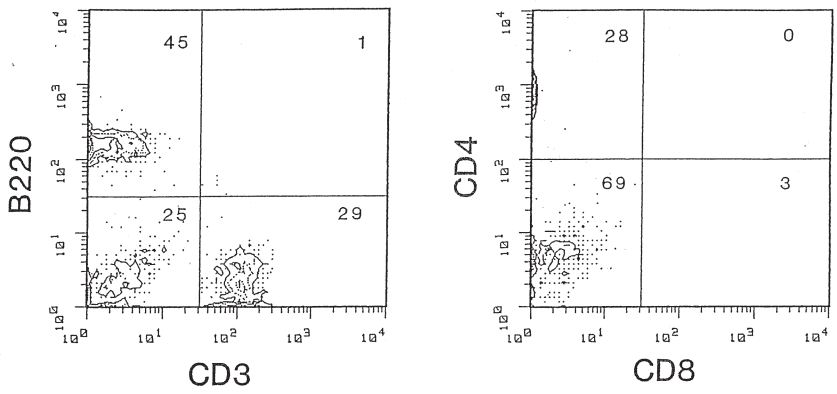

Fig. 3. Two color analysis of infiltrating lymphocytes in mandibular gland from a 12 month-old female mouse. Analysis of T cells (CD3+) and B cells (B220+) ratio (left) and CD4+ and CD8+ T cells subsets (right). Percentage of each gated cells are shown at upper right corner.

autoantibody is absent in most SS patients [3, 21, 26], indicating that the antibody may not play a primary role in pathogenesis.

In conclusion, sialadenitis in IQI/Jic mice coincide with the features of human SS in many respects. This mouse strain may be a novel animal model to clarify the pathological mechanism of SS.

ACKNOWLEDEMENT. We particularly wish to thank Dr. A. Yasuda at the Laboratory of Experimental Toxicology in this institute for his technical support in flow cytometric analysis.

REFERENCES

1. Adamson, T. C., Fox, R. I., Frisman, D. M., and Howell, F. V. 1983. Immunohistologic analysis of lymphoid infiltrates in primary Sjögren's syndrome using monoclonal antibodies. *J. Immunol.* 130: 203–208.
2. Chused, T. M., Hardin, J. A., Frank, M. M., and Green, I. 1974. Identification of cells infiltrating the minor salivary glands in patients with Sjögren's syndrome. *J. Immunol.* 112: 641–648.
3. Fox, R. I. and Kang, H. I. 1993 Sjögren's syndrome: An autoimmune exocrinopathy. pp. 317–332. *In*: The Molecular Pathology of Autoimmune Diseases (Bona, C. A., Siminovitch, K. A., Zanetti, M., and Theofilopoulos, A. N. eds.), Harwood Academic Publishers.
4. Fujiwara, K., Sakaguchi, N., and Watanabe, T. 1991 Sialoadenitis in experimental graft-versus-host disease. An animal model of Sjögren's syndrome. *Lab. Invest.* 65: 710–718.
5. Green, J. E., Hinrichs, S. H., Vogel, J., and Jay, G. 1989. Exocrinopathy resembling Sjögren's syndrome in HTLV-1 tax transgenic mice. *Nature (Lond.)* 341: 72–74.
6. Haneji, N., Hamano, H., Yanagi, K., and Hayashi, Y. 1994. A new animal model for primary Sjögren's syndrome in NFS/sld mutant mice. *J. Immunol.* 153: 2769–2777.
7. Hayashi, Y., Kurashima, C., Utsuyama, M., and Hirokawa, K. 1988. Spontaneous development of autoimmune sialadenitis in aging BDF1 mice. *Am. J. Pathol.* 132: 173–179.
8. Hayashi, Y., Utsuyama, M., Kurashima, C., and Hirokawa, K. 1989 Spontaneous development of organ-specific autoimmune lesions in aged C57BL/6 mice. *Clin. Exp. Immunol.* 78: 120–126.
9. Hayashi, Y., Deguchi, H., Nakahata, A., Kurashima, C., Utsuyama, M., and Hirokawa K. 1990. Autoimmune sialadenitis: Possible models for Sjögren's syndrome and a common aging phenomenon. *Autoimmunity* 5: 215–228,
10. Hoffman, R. W., Alspaugh, M. A., Waggie, K. S., Durham, J. B., and Walker, S. E. 1984 Sjögren's syndrome in MRL/l and MRL/n mice. *Arth. Rheum.* 27: 157–165.
11. Horsfall, A. C., Rose, L. M., and Maini, R. N. 1989. Autoantibody synthesis in salivary glands of Sjogren's syndrome patients. *J. Autoimmun.* 2: 559–568.
12. Horsfall, A. C., Skarstein, K., and Jonnson, R. 1994. Experimental models of Sjögren's syndrome. pp. 67–88. *In*: Autoimmune Disease: Focus on Sjögren's Syndrome (Isenberg,D.A. and Horsfall, A.C. eds.). BIOS Scientic Publishers.
13. Isenberg, D. A., Rowe, D., Tookman, A., Hopp, A., Griffiths, M., Paice, E., Stewart, J., and Beverley, P. C. L. 1984. An immunohistological study of secondary Sjögren's syndrome. *Ann. Rheum. Dis.* 43: 470–476.
14. Jabs, D. A. and Prendergost, R. A. 1988. Murine models of Sjögren's syndrome: Immunohistologic analysis of different strains. *Invest. Opthamol. Vis. Sci.* 29: 1437–1443.
15. Jonnson, R. and Holmdahl, R. 1990. Infiltrating mononuclear cells in salivary glands and kidney in autoimmune MRL/Mp-lpr/lpr mice express IL 2 receptor and produce interferon γ. *J. Oral. Pathol. Med.* 19: 330–334.
16. Jonsson, R. and Mountz, J. 1993. Experimental models of Sjögren's syndrome. pp. 333–345. *In*: The Molecular Pathology of Autoimmune Diseases (Bona, C. A., Siminovitch, K. A., Zanetti, M., and Theofilopoulos, A. N. eds.), Harwood Academic Publishers.
17. Jonsson, R., Pitts, A., Mestecky, J., and Koopman, W. 1991. Local IgA and IgM rheumatoid factor production in autoimmune MRL/lpr mice. *Autoimmunity* 10: 7–14.
18. Jonsson, R., Tarkowski, A., Backman, K., and Klareskog, L. 1987. Immunohistochemical characterization of sialadenitis in NZB x NZW F1 mice. *Clin. Immunol. Immunopathol.* 42: 93–101.
19. Jonsson, R., Tarkowski, A., Backman, K., Holmdahl, R., and Klareskog, L. 1987. Sialadenitis in the MRL-1 mouse: Morphological and immunohistochemical characterization of resident and infiltrating cells. *Immunology* 60: 611–616.
20. Kato, H. 1989. Animal models derived from the ICR mouse for human diseases. *Med. Immunol.* 17: 353–361 (in Japanese).
21. Kauseman, D., Allen, M. E., Snaith, M. L., and Isenberg, D. A. 1994. Autoimmunity and the clinical spectrum of Sjögren's syndrome. pp. 1–24. *In*: Autoimmune Diseases: Focus on Sjögren's Syndrome (Isenberg, D. A. and Horsfall, A. C. eds.), BIOS Scientic Publishers.
22. Kessler, H. 1968. A laboratory model for Sjögren's syndrome. *Am. J. Pathol.* 52: 671–685.
23. Lane, H. C., Callihan, T. R., Jaff, E. S., Fauci, A. S., and Moutsopoulos, H. M. 1983. Presence of intracytoplasmic IgG in the lymphocytic infiltrates of the minor salivary glands of patients with primary Sjögren's syndrome. *Clin. Exp. Rheumatol.* 1: 237–239.
24. Lindahl, G., Hedfors, E., Klareskog, L., and Forsum, U. 1985. Epithelial HLA-DR expression and T lymphocyte subsets in salivary glands in Sjögren's syndrome. *Clin. Exp. Immunol.* 61: 475–482.
25. Miyagawa, J., Hanafusa, T., Miyazaki, A., Yamada, K., Fujino-Kurihara, H., Nakajima, H., Kono, N., Nonaka, K., Tochino, Y., and Tarui, S. 1986. Ultrastructual and immunocytochemical aspects of lymphocytic submandibulitis in the non-obese diabetic (NOD) mouse. *Virchow Arch [Cell Pathol]* 51: 215–225.
26. Moutsopoulos, H. M., Tzioufas, A. G., and Talal, N. 1991. Sjögren's syndrome: A model to study autoimmunity and lymphoid malignancy. pp. 319–340. *In*: Molecular Autoimmunity (Talal, N. ed.), Academic Press.
27. Saegusa, J., Kiuchi, Y., and Itoh, T. 1990. Antinucleolar autoantibody induced in mice by mercuric chloride. Strain difference in susceptibility. *Exp. Anim. (Tokyo)* 39: 597–599.
28. Saegusa, J., Yasuda, A., and Kubota, H. 1996. IQI/Jic mice have thymic B cells. *Exp. Anim. (Tokyo)* 45: 353–360.
29. Scott, J., Wolff, A., and Fox, P. C. 1990 Histologic assessment of the submandibular glands in autoimmune-disease-prone mice. *J. Oral Pathol. Med.* 19: 131–135.
30. St. Clair, E. W., Kenan, D., Burch, J. A., Keene, J. D., and

Pisetsky, D. S. 1991. Anti-La antibody production by MRL-lpr/lpr mice. Analysis of fine specificity. *J. Immunol.* 146: 1885–1892.

31. Suzuki, K., Makino, M., Okada, Y., Kinoshita, J., Yui, R., Kanazawa, H., Asakura, H., Fujiwara, M., Mizuochi, T., and Komuro, K. 1993. Exocrinopathy resembling Sjögren's syndrome induced by a murine retrovirus. *Lab. Invest.* 69: 430–435.

32. Talal, N., Sylvester, R. A., Daniels, T. E., Greenspan, J. S., and Williams, R. C. 1974. T and B lymphocytes in peripheral blood and tissue lesions in Sjögren's syndrome. *J. Clin. Invest.* 53: 180–189.